TOR VERGATA
UNIVERSITÀ DEGLI STUDI DI ROMA

NISSAN

INTERNATIONAL CAE CONFERENCE

FEA Shape Optimization of a Nissan Micra Front Subframe

Emanuele Di Meo, RINA Consulting S.p.A.
Claudio Ponzo, Nissan Technical Centre Europe
Prof. Marco E. Biancolini, University of Rome "Tor Vergata"

38th International CAE Conference
November 16, 2022

Introduction

- The structural optimization of the front chassis and suspension lower arms of a Nissan Micra was performed
- The objective of the optimization was an increase of driving comfort and road holding
- Lateral stiffness was optimized acting on thickness and shape variation of subframe elements

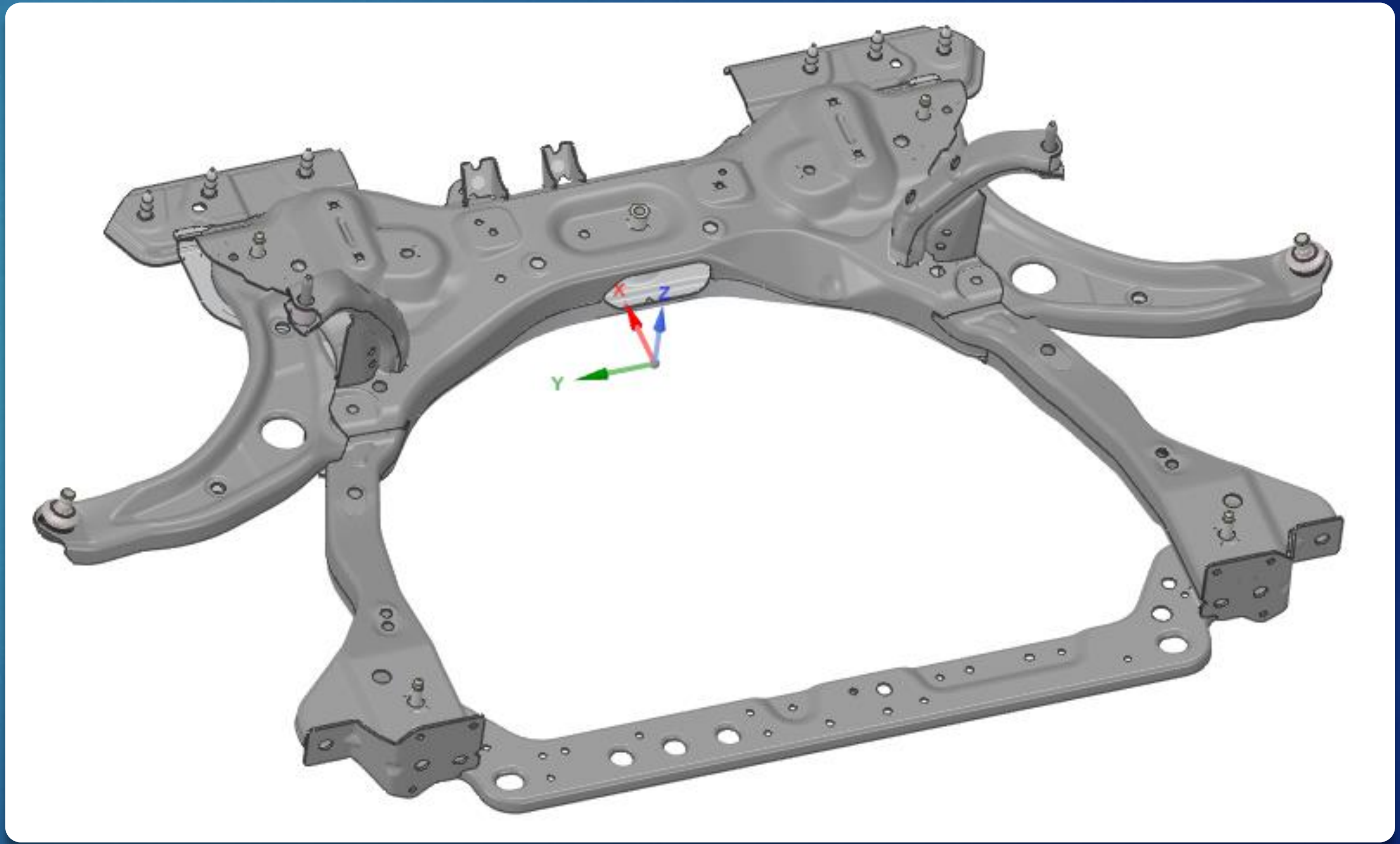

Nissan Micra

- Nissan Micra model K14
- B-segment car
- Fifth generation Micra
- Unveiled at 2016 Paris Motor Show
- On sale since March 2017
- Front-wheel transmission drive
- McPherson suspension

Front subframe

- Frame substructure connecting suspension to body
- Distributes loads coming from powertrain and suspensions to other areas of the body
- Isolates vibrations, being connected to the body through elastic bushings.
- Absorbs energy and body deformation in case of crash

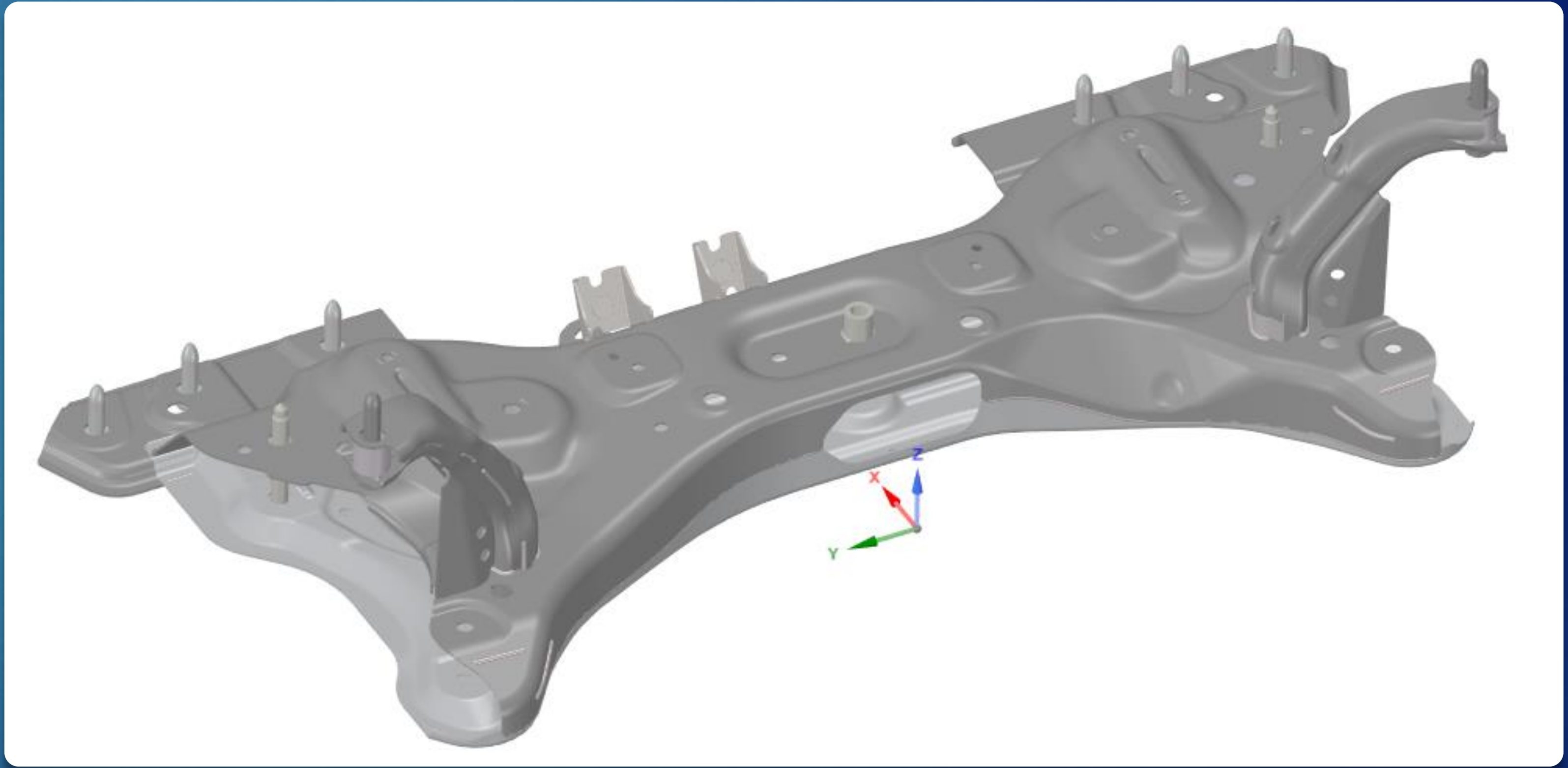

Emanuele Di Meo, *RINA Consulting S.p.A. -* ***Claudio Ponzo,*** *Nissan Technical Centre Europe -* ***Prof. Marco E. Biancolini,*** *University of Rome "Tor Vergata"*

Stiffness test

- Subframe structure including mounts and suspension lower arms is mounted on a rig
- Assembly is loaded by hydraulic cylinder acting on the ball joint connecting lower arm to wheel
- LVDTs (Linear variable differential transformers) measure deflection in areas of concern

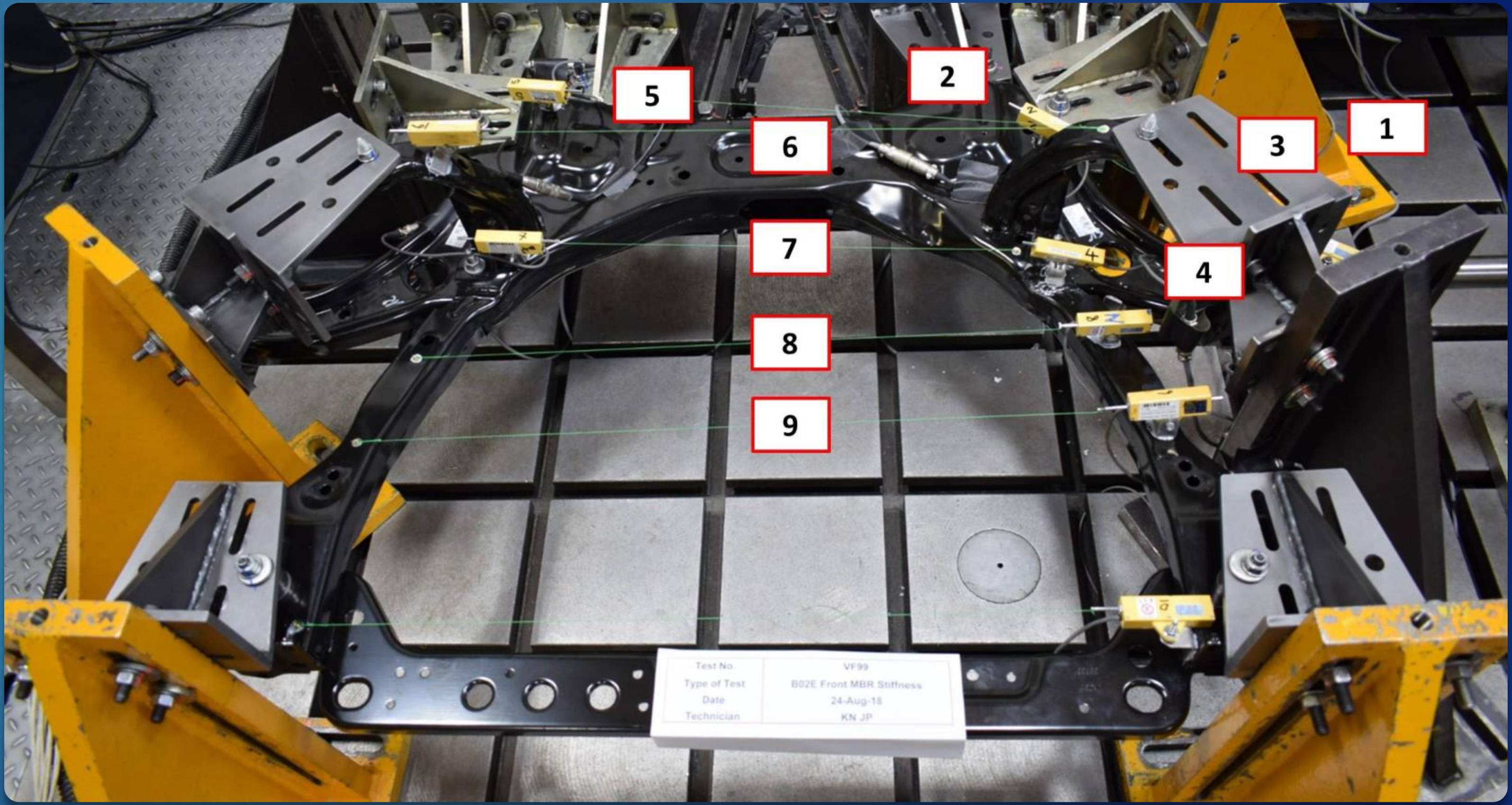

Emanuele Di Meo, *RINA Consulting S.p.A. -* ***Claudio Ponzo,*** *Nissan Technical Centre Europe -* ***Prof. Marco E. Biancolini,*** *University of Rome "Tor Vergata"*

Stiffness test

- Subframe structure including mounts and suspension lower arms is mounted on a rig
- Assembly is loaded by hydraulic cylinder acting on the ball joint connecting lower arm to wheel
- LVDTs (Linear variable differential transformers) measure deflection in areas of concern

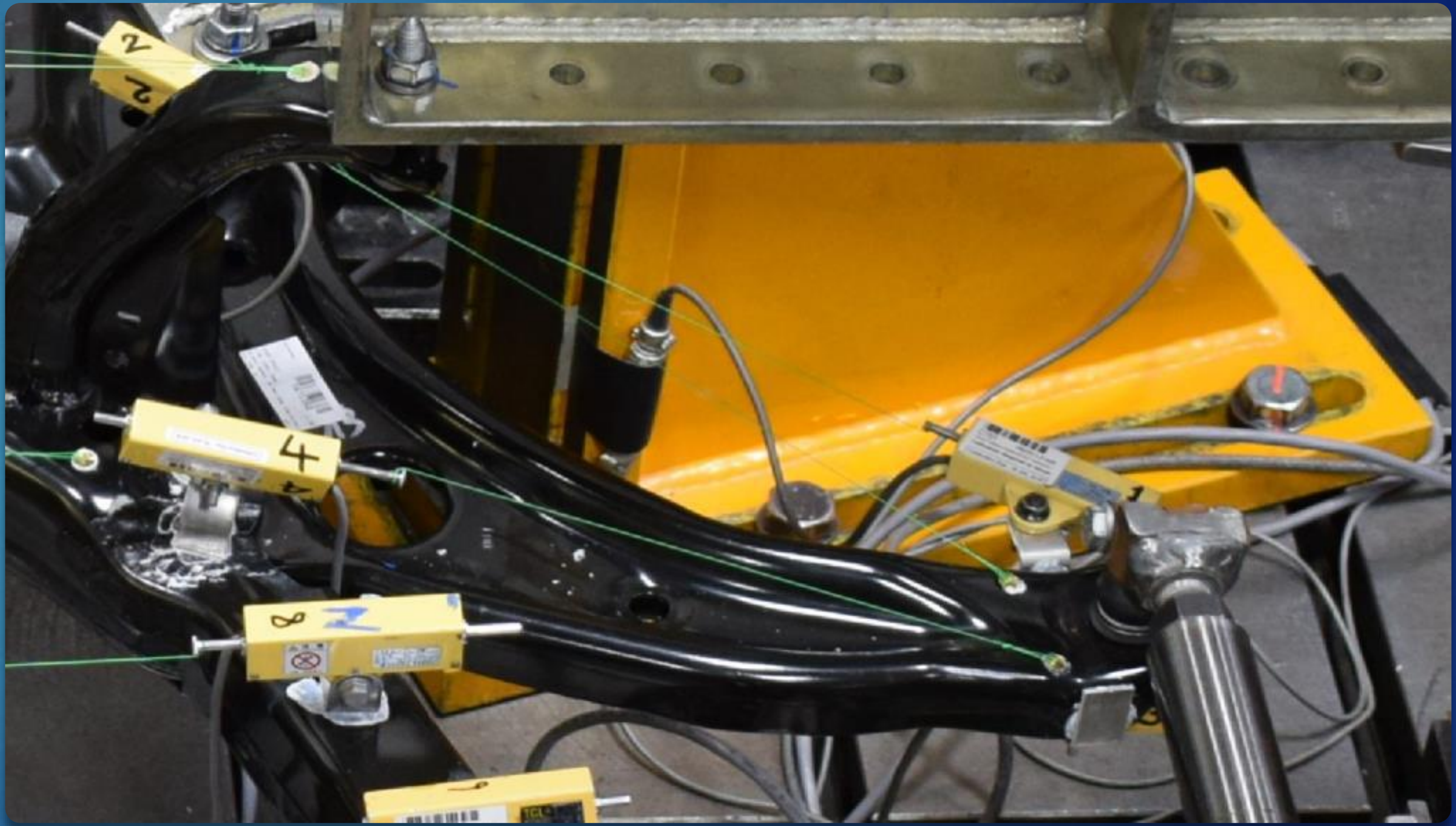

Finite element study

- Geometry
- Meshing
- Material, constraints, loads
- Analysis and results evaluation
- Comparison and matching with experimental data
- Shape optimization

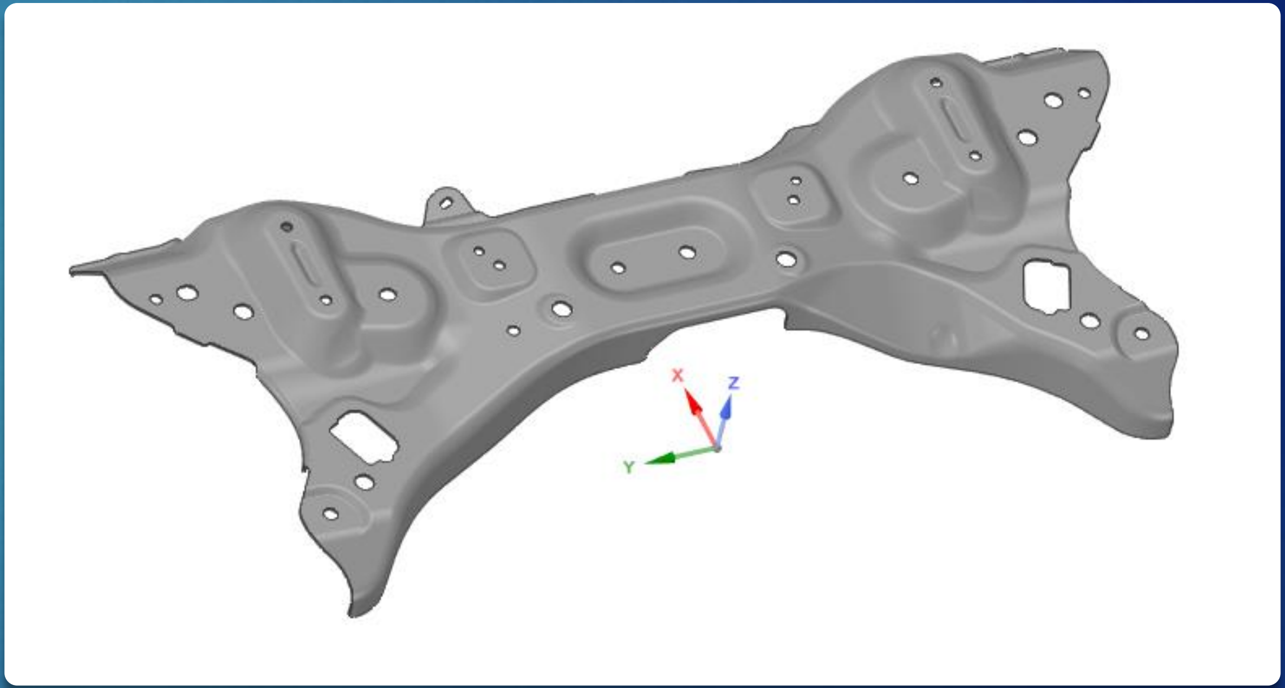

Geometry simplification

- Original CAD needs to be simplified before meshing
- Midsurfacing
- Surface merging to remove small surfaces
- High order NURBS surface relaxation
- Testing and validation applying a lateral and longitudinal load

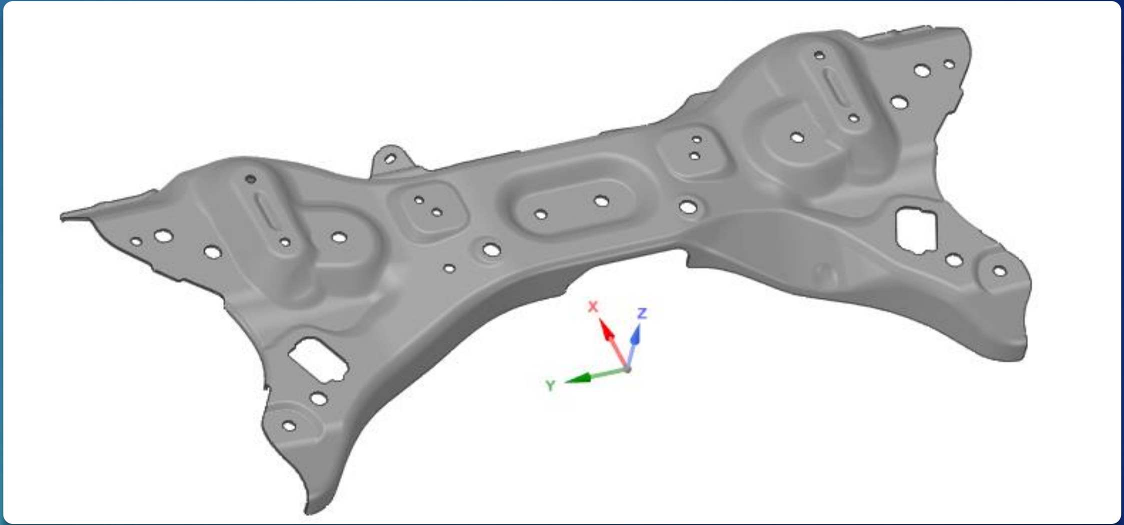

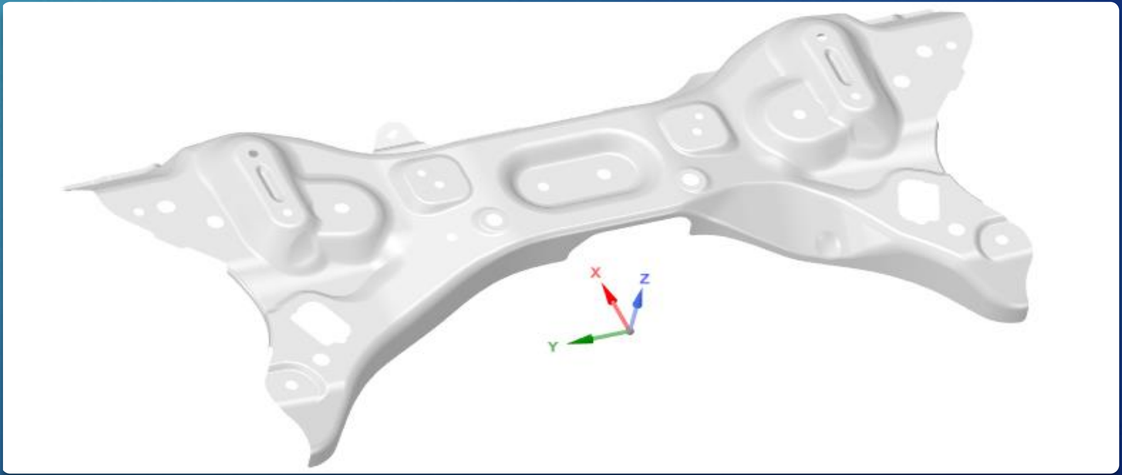

Meshing

- Triangular shell elements
- Linear elements
- 107,660 nodes
- 207,178 elements
- Different mesh sizing

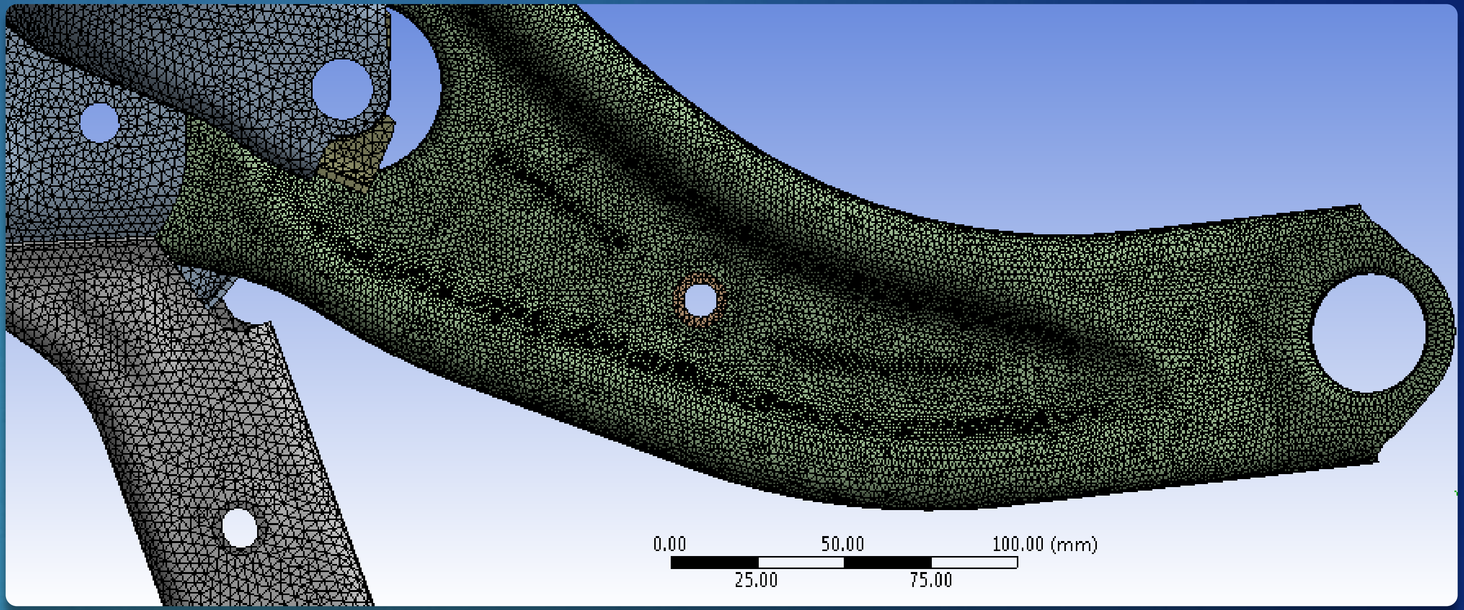

Area of concern	Mesh sizing
General sizing	6 mm
Front member (on the right)	3.2 mm
Lower arms	2.4 mm
Weld surfaces	0.6 mm
Welded connection areas	1.2 mm

Material

- Steel made front subframe
- Properties in table

Property	Value
Density	7850 kg/m^3
Young's Modulus	2E+11 Pa
Poisson's ratio	0.3
Shear Modulus	7.69E+10 Pa
Tensile Yield Strength	2.5E+8
Compressive Yield Strength	2.5E+8
Tensile Ultimate Strength	4.6E+8

Constraints

- Bolts connect subframe to main frame or body
- Projecting bolts contact areas on the subframe, red areas are obtained
- Such red areas are set as fixed

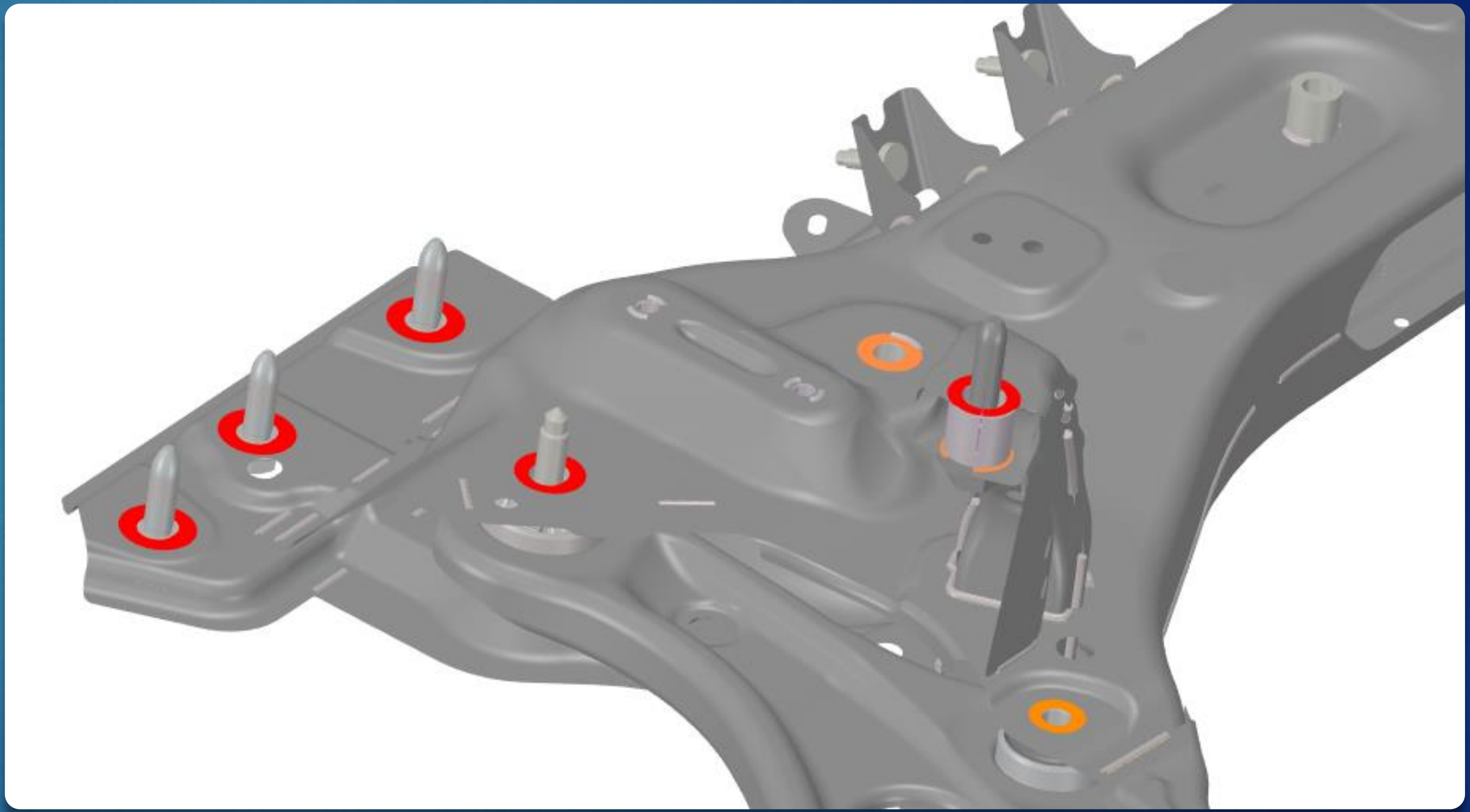

Connections

- Single parts of the structure are connected by welds or bushes
- Spot welds connect close parts and are modelled in two different ways
- Bushings connect lower arms to subframe

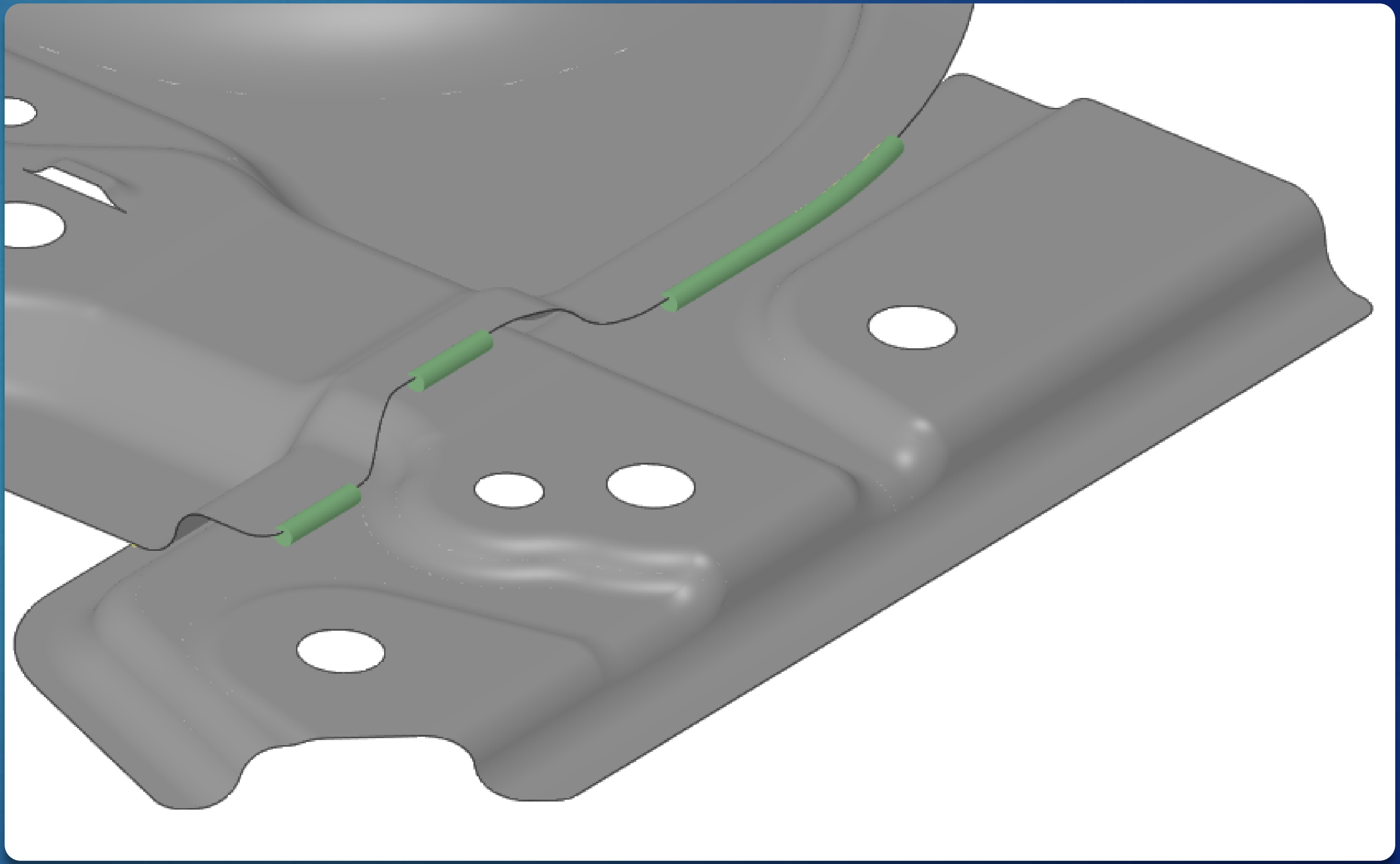

Welds

- Two cases: edge or corner joints
- Edge joints are modelled through bonded connections acting at geometry level
- Corner joints are modelled through mesh connections acting at mesh level
- In both cases, weld geometry is not modelled.

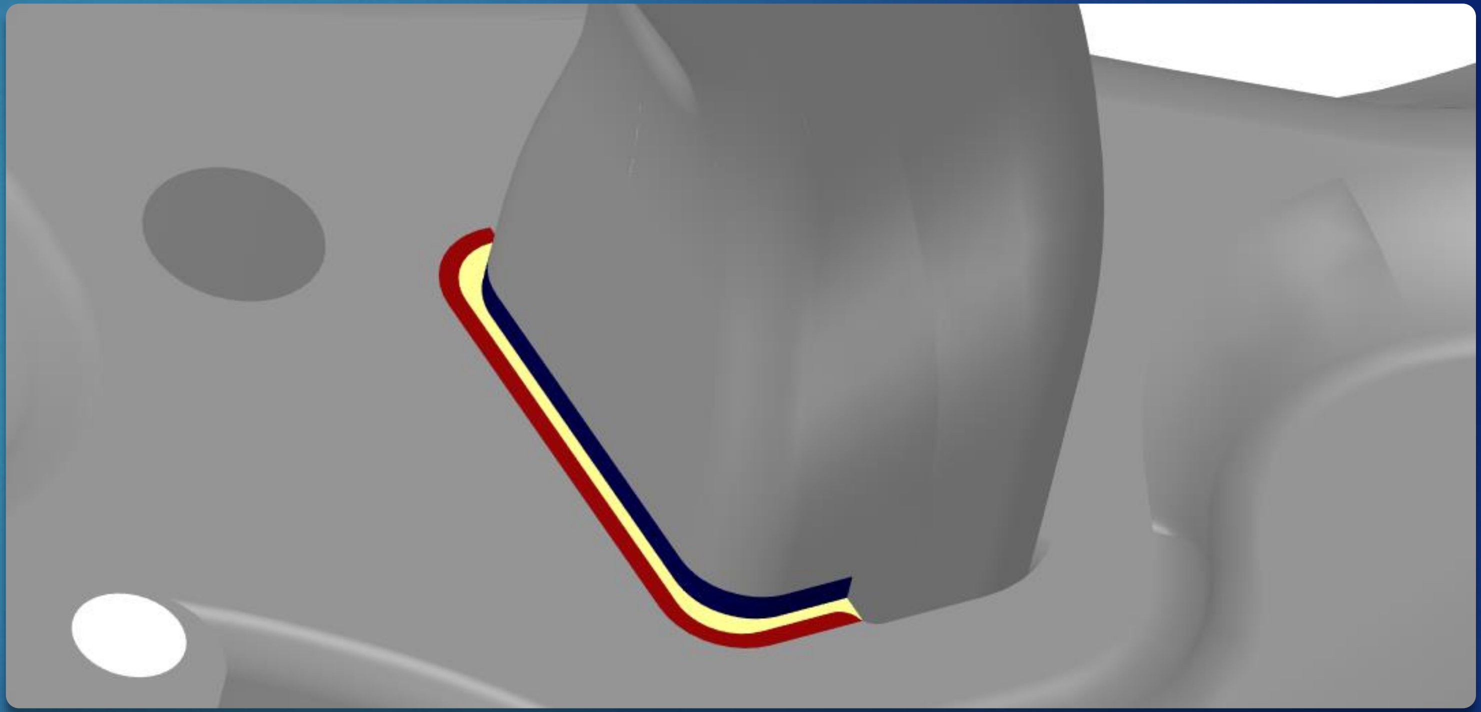

Bushings

- Flexible bushings connect suspension lower arm to the subframe
- Experimental data to be extrapolated are given
- Stiffer bushing for road holding, more flexible for comfort
- Four stiffness curves characterize each bushing

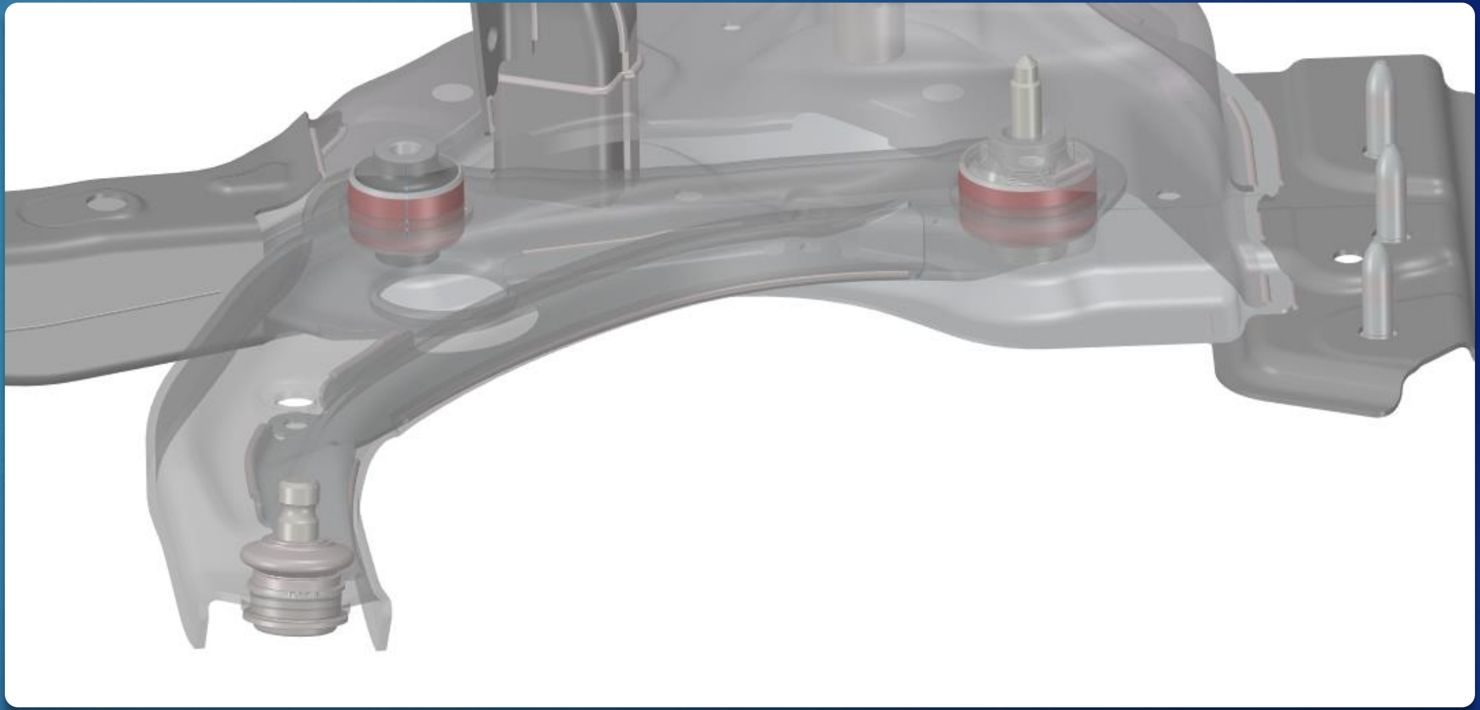

Bushings stiffness

- Radial, Axial, Conical, Torsional
- Stiffening and hysteresis behaviour
- No mutual interaction
- Represented by a polynomial curve

$F_i = k_0 + k_1 x_i^{n1} + k_2 x_i^{n2} + k_3 x_i^{n3} + \dots$

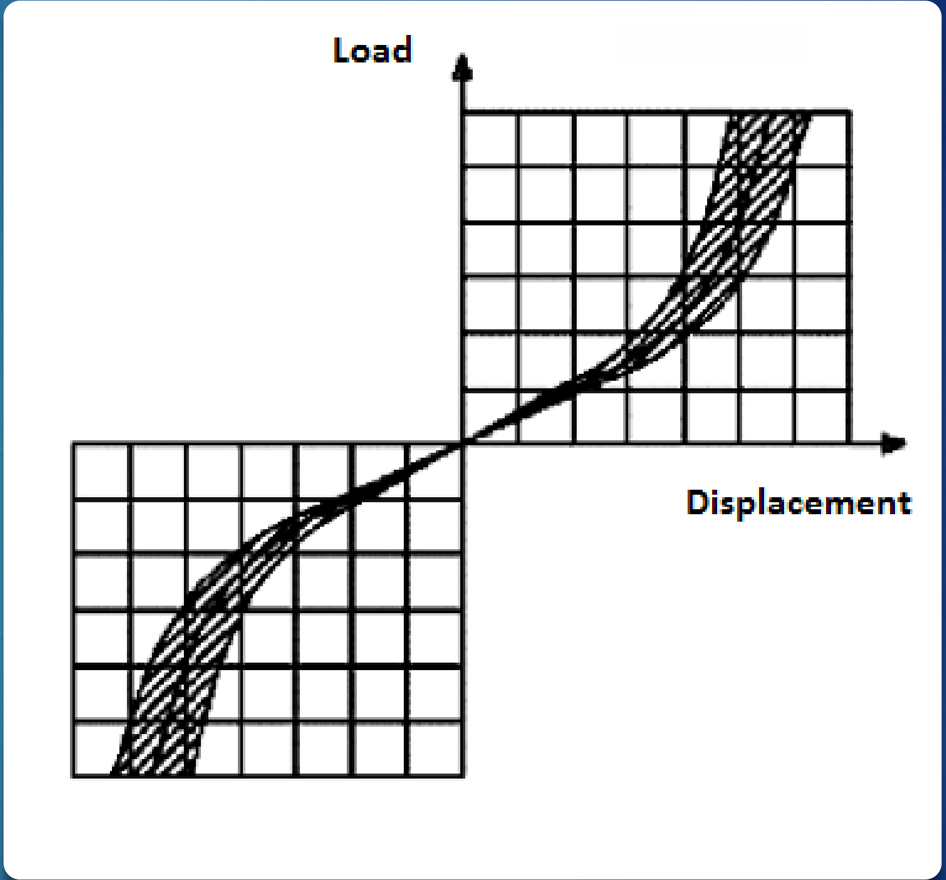

Load conditions

- Load by hydraulic cylinder is applied on the ball joint
- Ball joints are not modelled in finite element analysis
- Load is directly applied on lower arm surface

Longitudinal Force (X)		Lateral Force (Y)	
$F_{1,LONG}$	-10883 N	$F_{1,LAT}$	-10313 N
$F_{2,LONG}$	-4712 N	$F_{2,LAT}$	-2755 N
$F_{3,LONG}$	4707 N	$F_{3,LAT}$	3032 N
$F_{4,LONG}$	11023 N	$F_{4,LAT}$	10284 N

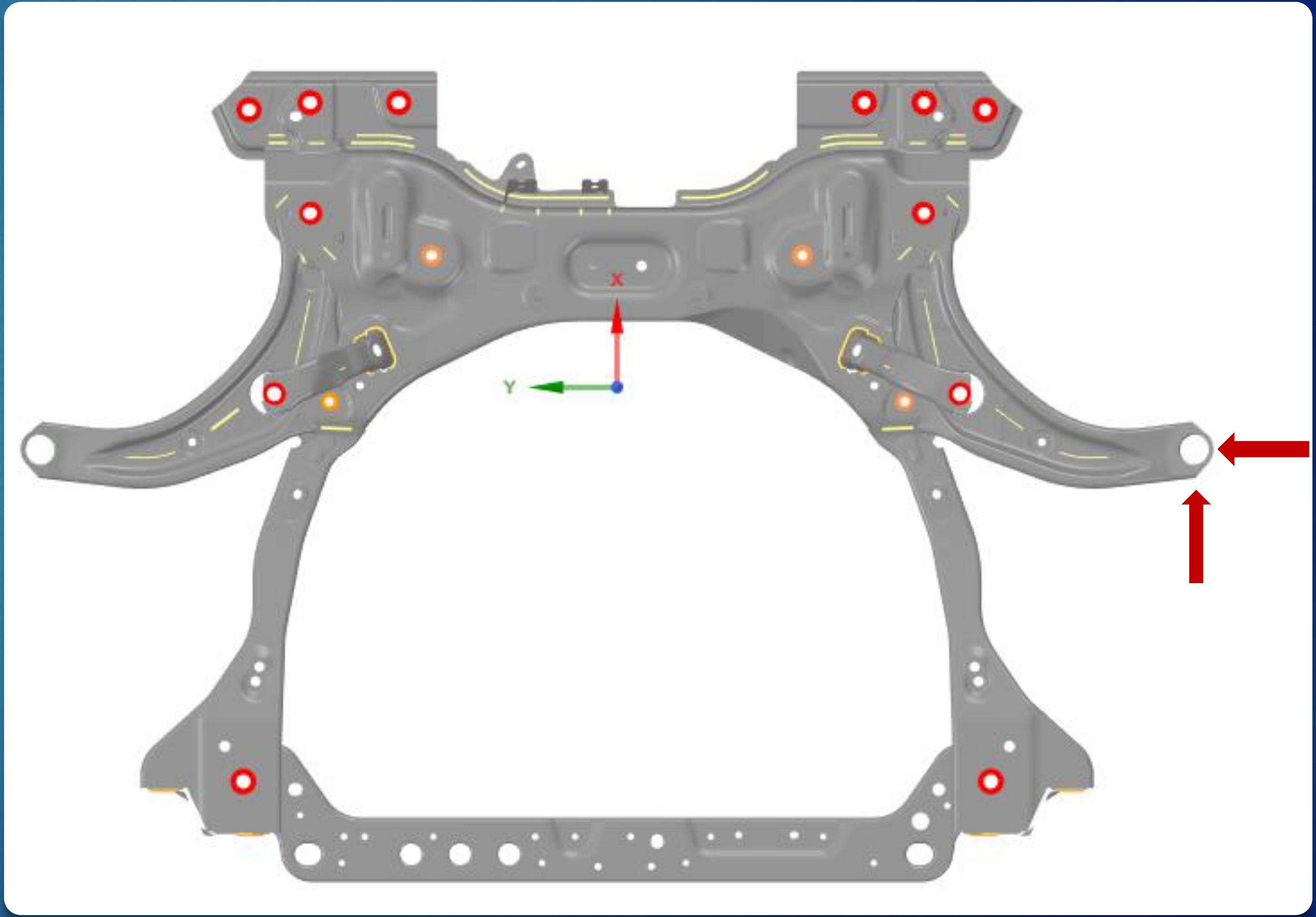

Analysis settings

- Non linear analysis performed due to complete bushing model
- Newton-Raphson with line search method
- Initial time sub-step: 0.1s

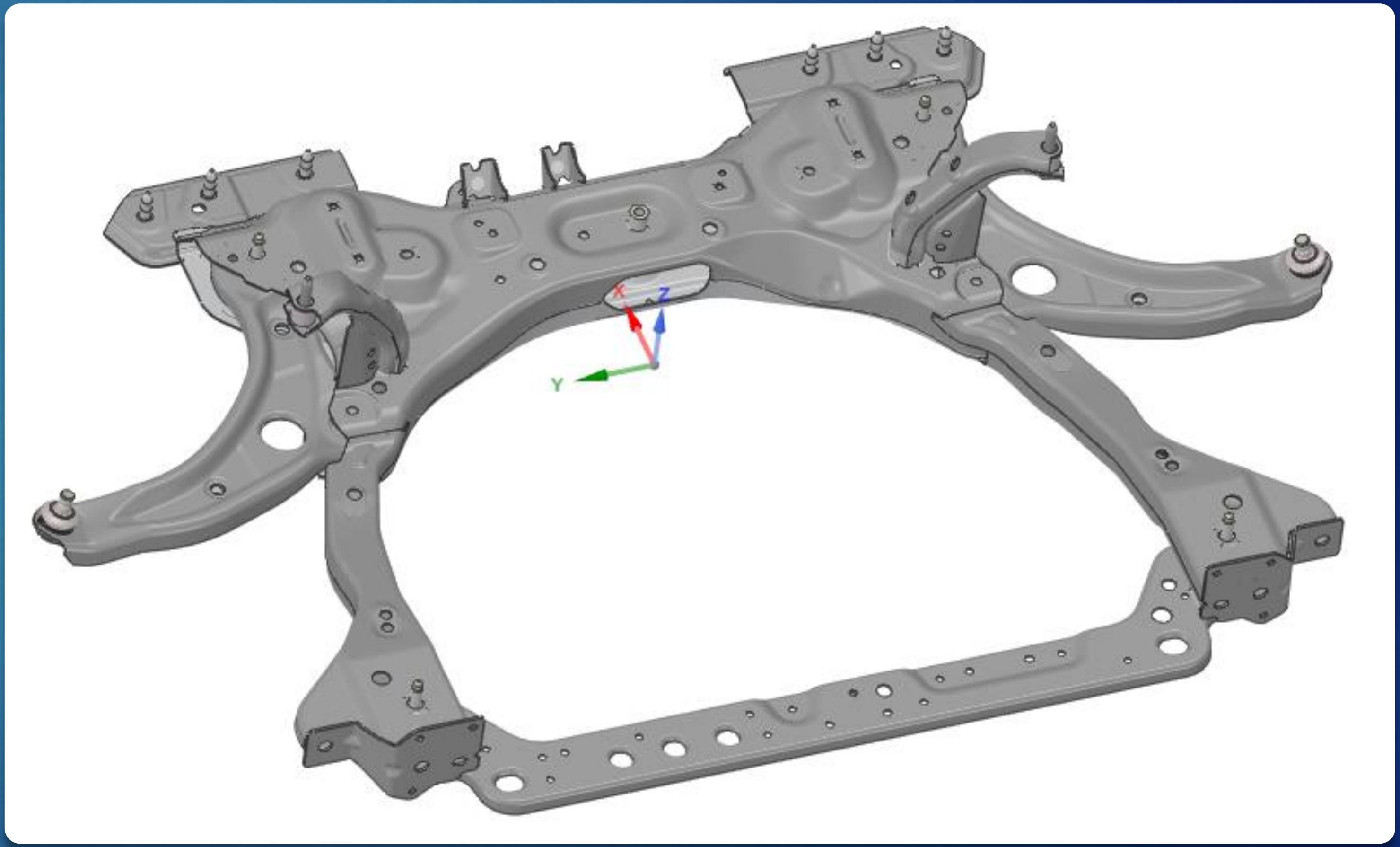

Emanuele Di Meo, *RINA Consulting S.p.A. -* ***Claudio Ponzo,*** *Nissan Technical Centre Europe -* ***Prof. Marco E. Biancolini,*** *University of Rome "Tor Vergata"*

Baseline Results

- LVDTs 2, 4 and 7 results are selected as the most important and their deflection results are compared to experimental data
- Mean stiffness is calculated as the ratio of applied force and deflection for each area of concern

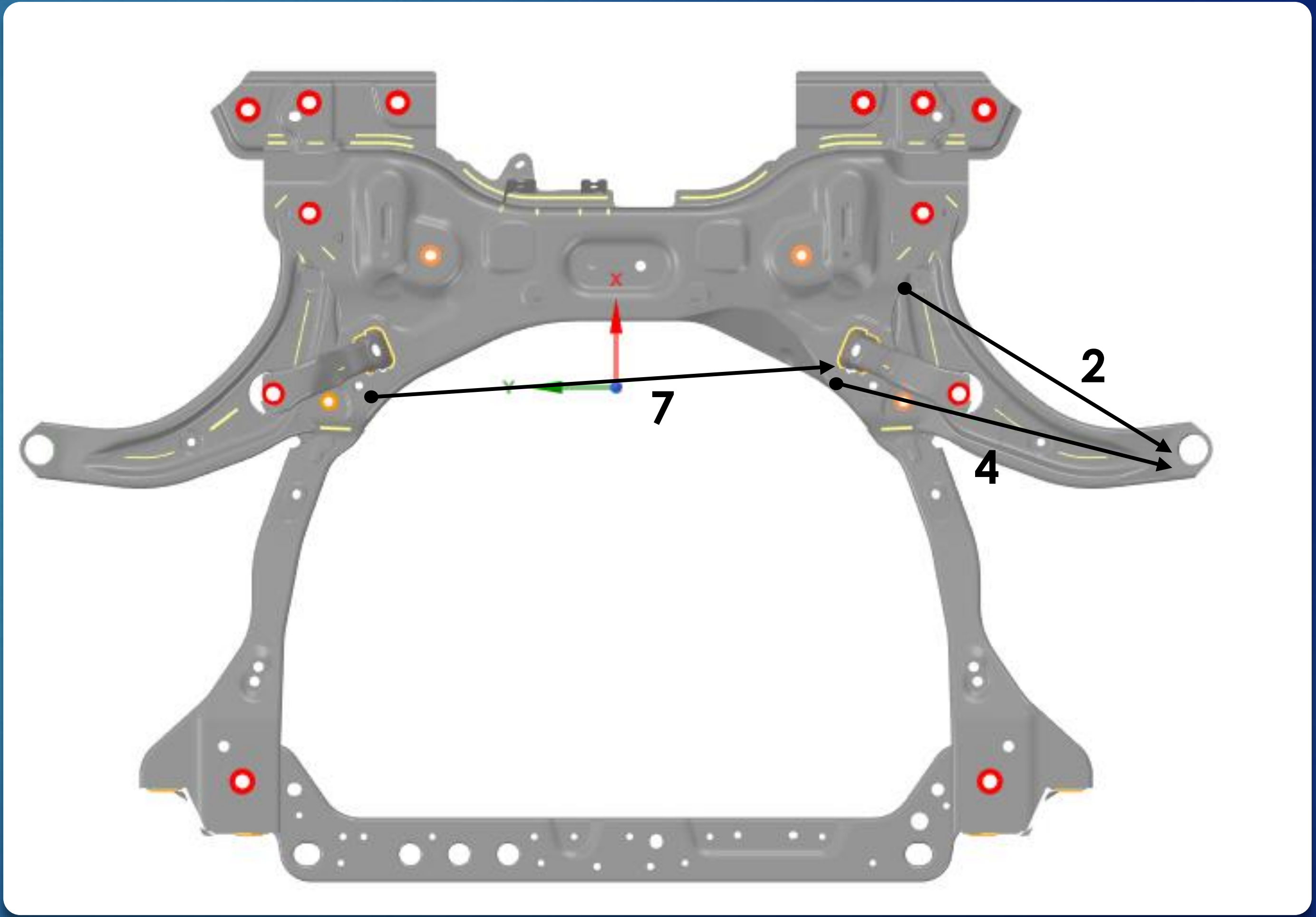

Baseline Results

- LVDTs 2, 4 and 7 results are selected as the most important and their deflection results are compared to experimental data
- Mean stiffness is calculated as the ratio of applied force and deflection for each area of concern

Stiff/Load	F_{LAT1}	F_{LAT2}	F_{LAT3}	F_{LAT4}	F_{LONG1}	F_{LONG2}	F_{LONG3}	F_{LONG4}
ΔL_2 [mm]	0.4109	0.1587	0.1522	0.3367	3.8803	3.4074	2.7339	2.2644
k_2 [kN/mm]	25.0971	17.3551	19.9219	30.5431	2.8047	1.3829	1.2717	4.8681
ΔL_4 [mm]	2.2428	1.1959	-1.0385	-1.608	-1.0589	-0.9144	6.1065	6.1994
k_4 [kN/mm]	4.5982	2.3035	2.919	6.3957	10.2777	5.1532	0.7708	1.7781
ΔL_7 [mm]	0.2457	0.0655	-0.0721	-0.2449	-0.3408	-0.1517	0.1515	0.3452
k_7 [kN/mm]	41.9779	42.0604	42.0611	41.9808	31.9384	31.0686	31.0681	31.9366

Structural Optimization

- Once the model is tuned with experimental data, the structure is optimized with the aim of improving lateral stiffness
- Bushes, lower arms and Q-link reinforcements are subject to a mixed parametric and morphing optimization

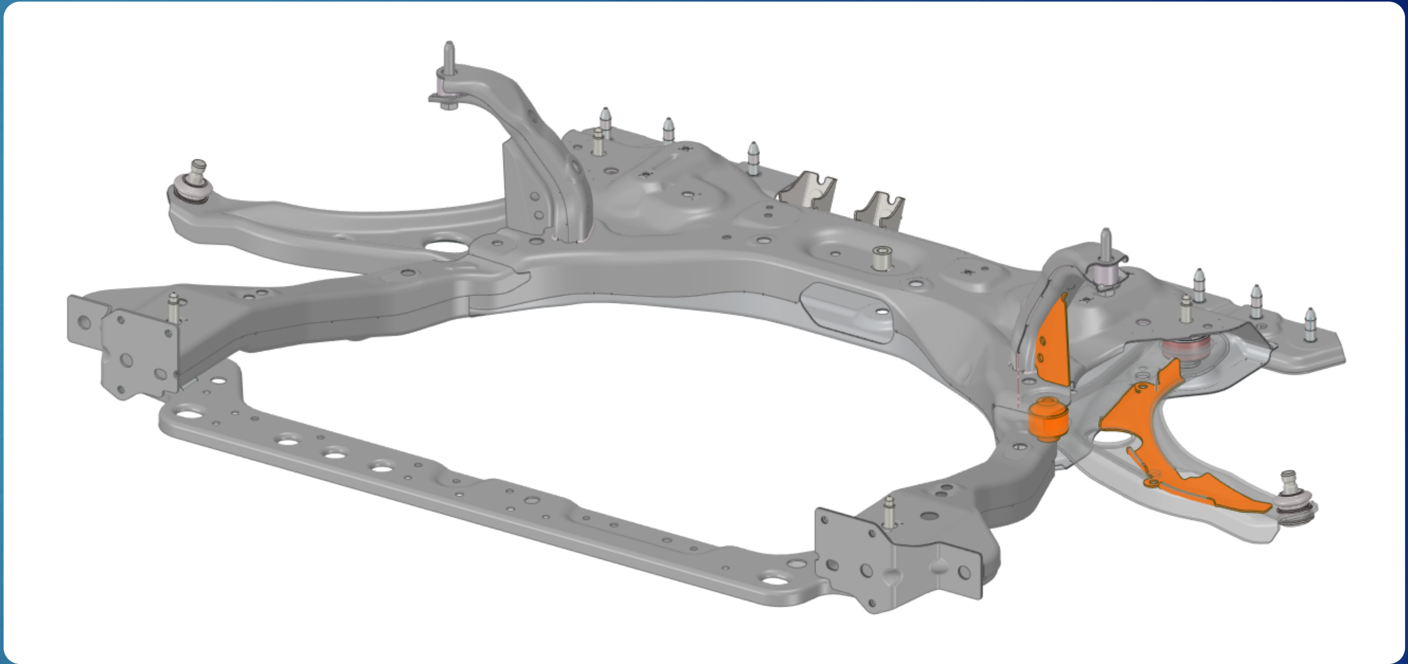

Structural Optimization

- Three areas of concern:
  - Front bush connecting body to TV-Link is replaced with a stiffer one
  - Lower arm reinforcement thickness is varied and beads added
  - Q-Link reinforcement shape is morphed

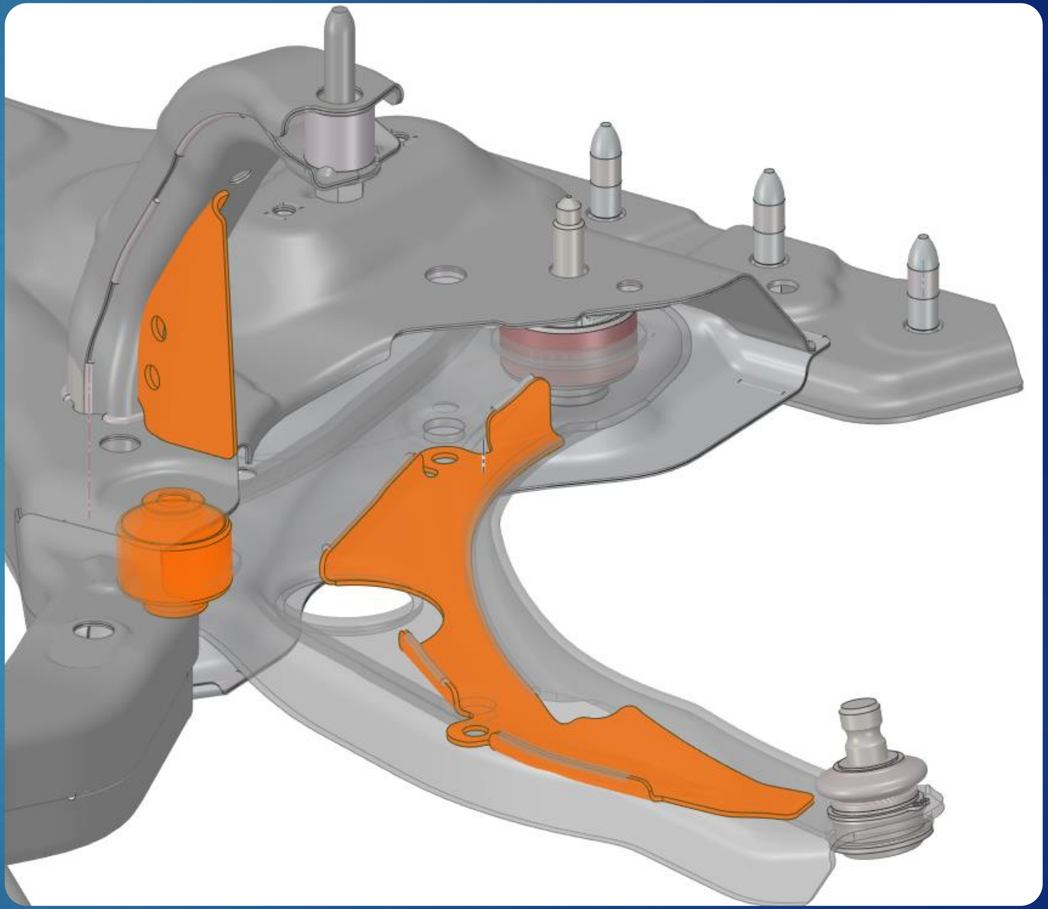

Structural Optimization: part 1

- In the first implementation a bush replacement is performed
- The central bush is replaced by another with higher stiffness parameters
- Shape modifications of bushing side are neglected

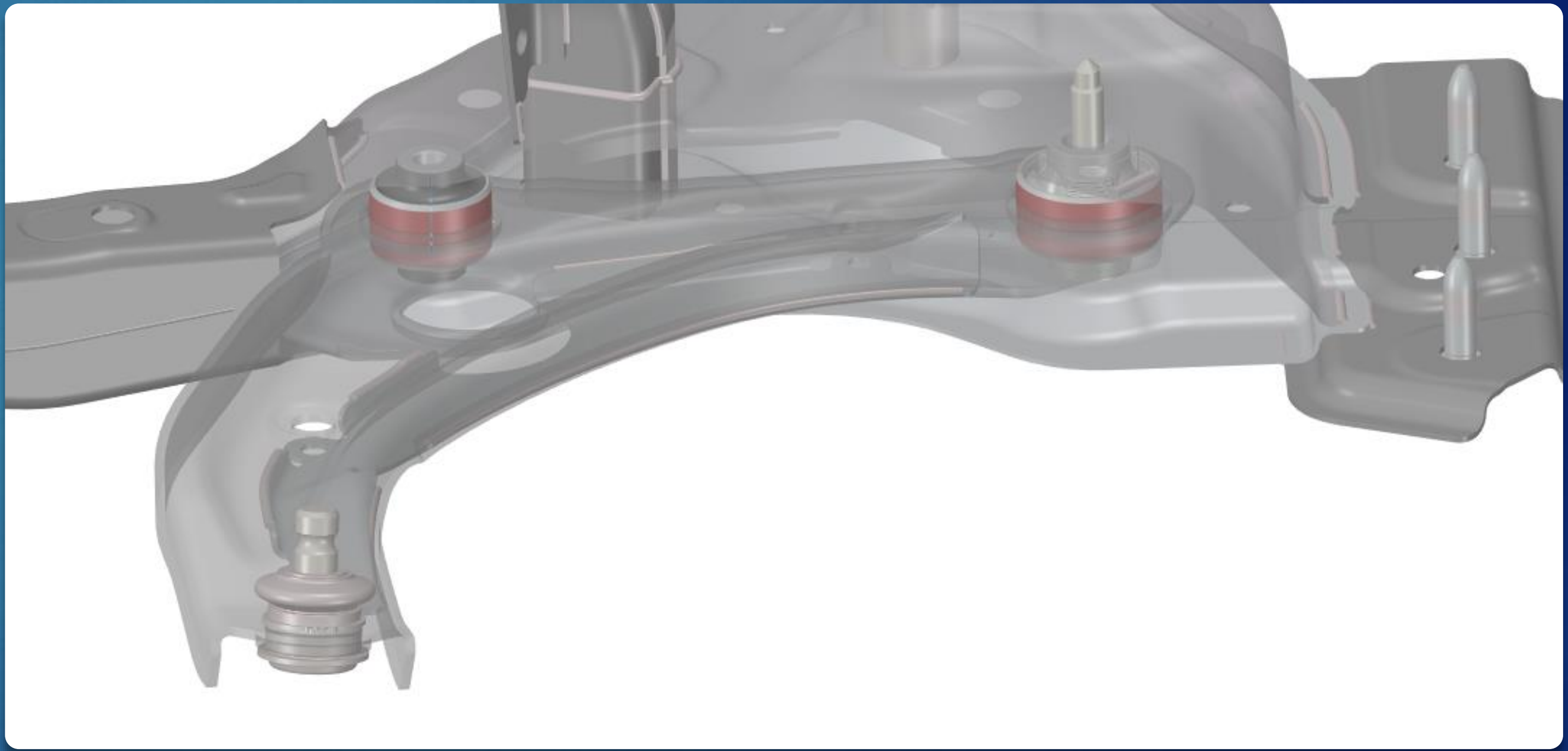

Emanuele Di Meo, *RINA Consulting S.p.A.* - ***Claudio Ponzo,*** *Nissan Technical Centre Europe* - ***Prof. Marco E. Biancolini,*** *University of Rome "Tor Vergata"*

NISSAN TOR VERGATA UNIVERSITÀ DEGLI STUDI DI ROMA

Structural Optimization: part 2

- In the second implementation, the lower arm reinforcement, highlighted in orange, is thickened, and beads are added through mesh morphing
- Reinforcement thickness is varied from the initial 2 mm value
- Each additional mm in reinforcement thickness causes a mass increase of 0,12857 kg

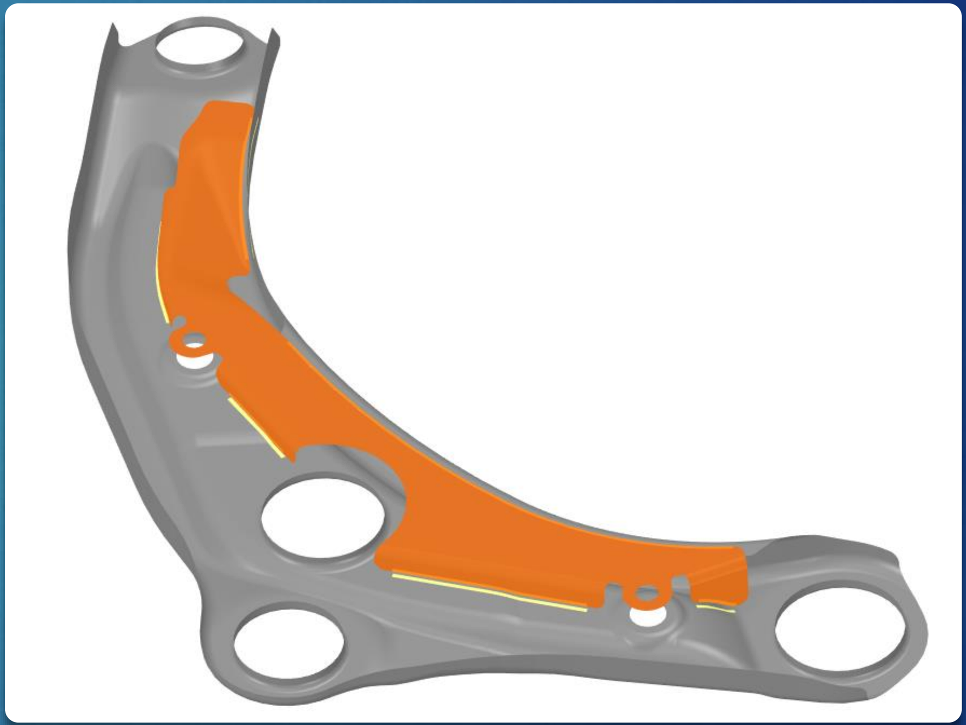

Structural Optimization: part 2

- The two contributions to stiffness of part thickness and beads are evaluated separately
- Thickness variations has a major effect on stiffness, but it also causes a weight increase

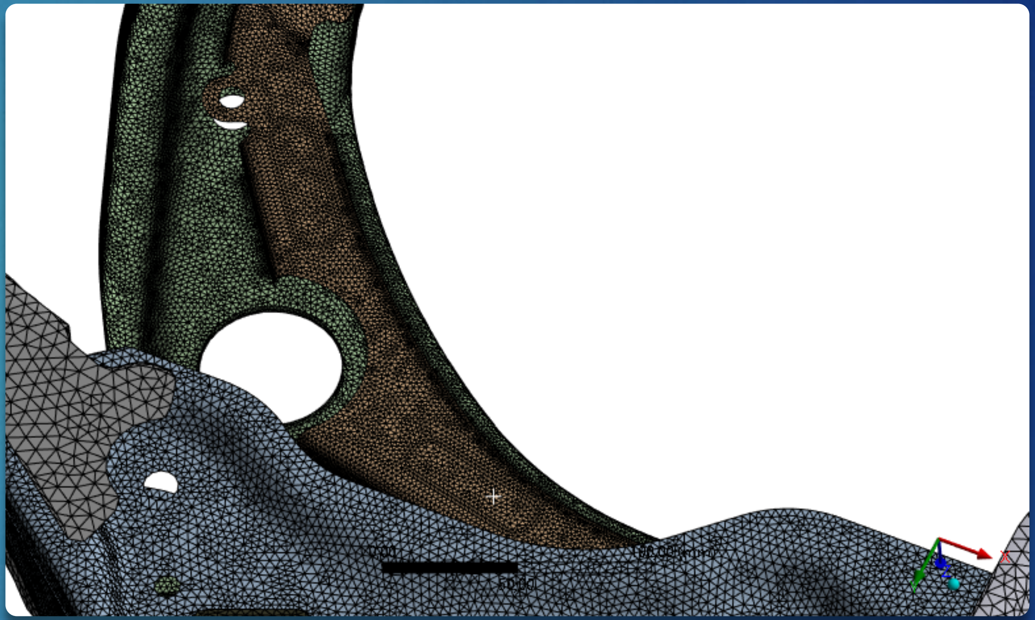

Structural Optimization: part 2

- Beads shape modification is performed through RBF mesh morphing
- In such a way it is possible to increase stiffness with negligible weight variation

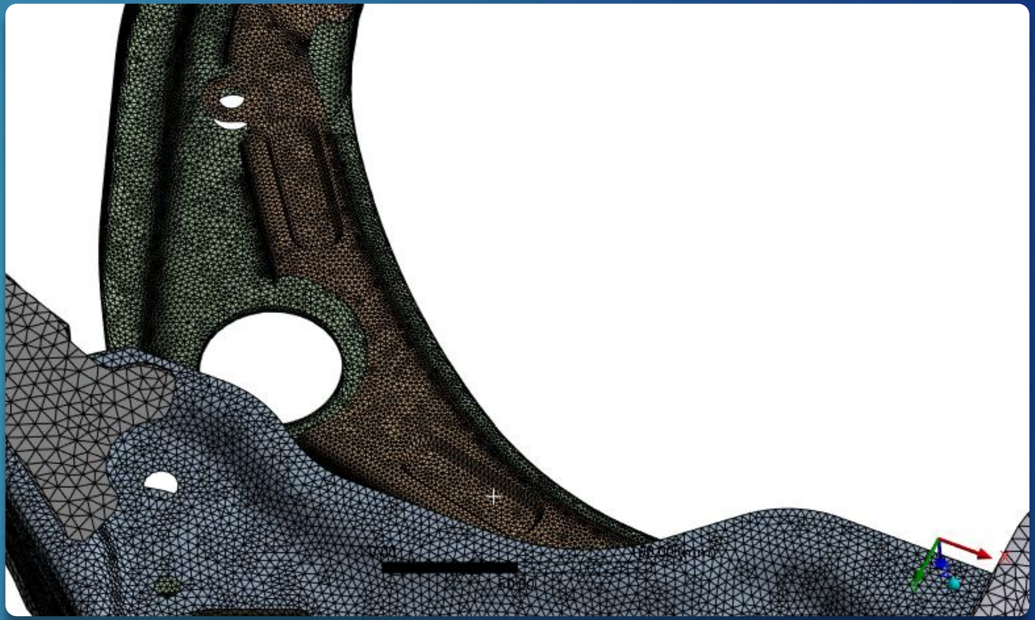

Emanuele Di Meo, *RINA Consulting S.p.A.* - ***Claudio Ponzo,*** *Nissan Technical Centre Europe* - ***Prof. Marco E. Biancolini,*** *University of Rome "Tor Vergata"*

Structural Optimization: part 3

- In the third test, Q-link reinforcement (highlighted in orange) is subject to a shape modification
- RBF mesh morphing is used to perform such a shape optimization

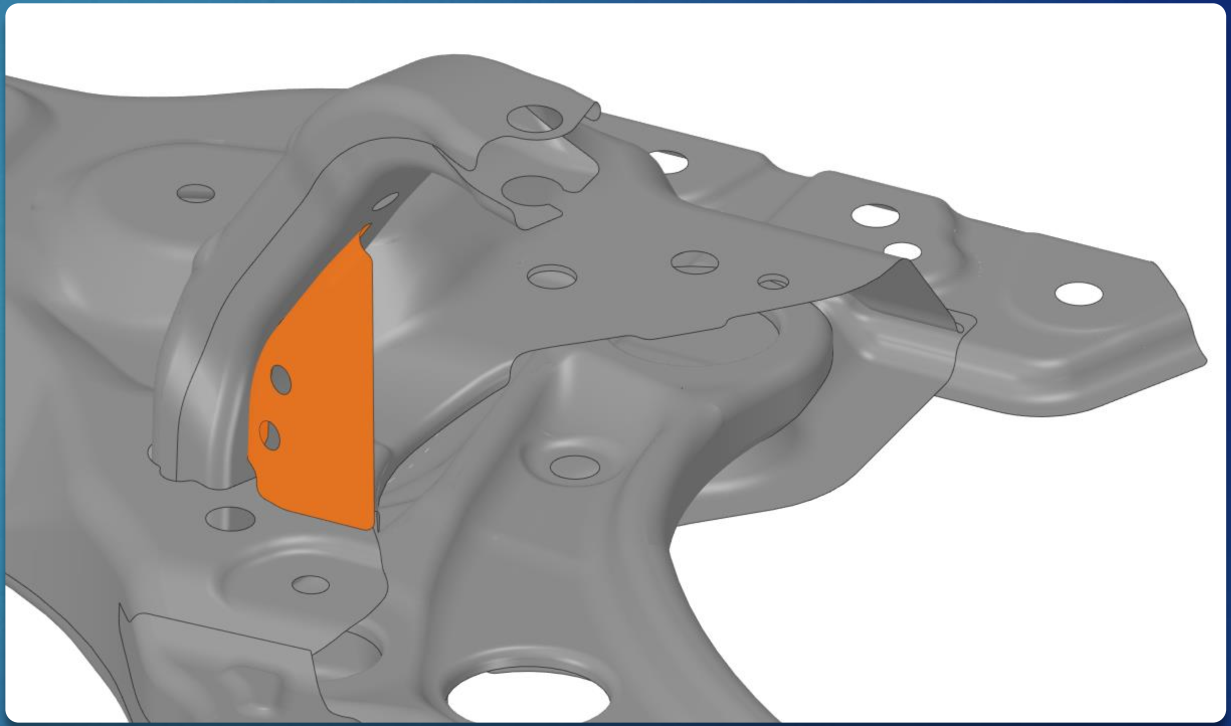

Structural Optimization: part 3

- Q-link reinforcement plays an important role in upper links stiffness
- It also contributes to lower body stiffness

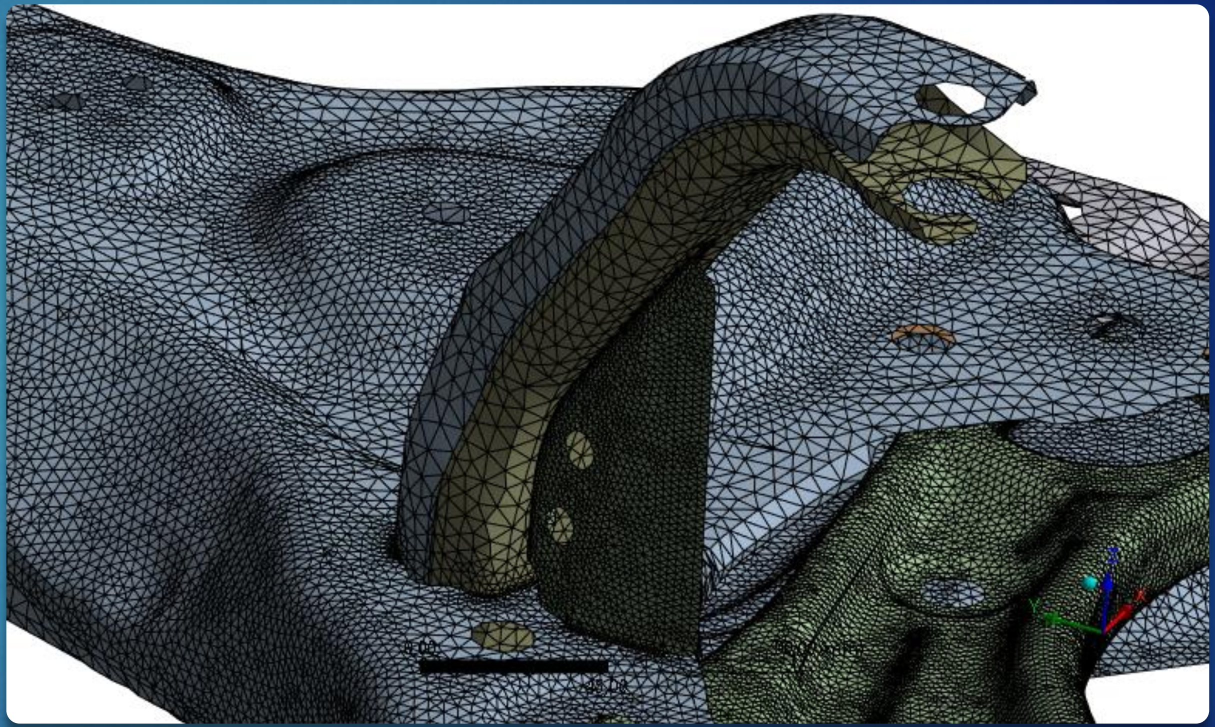

Emanuele Di Meo, *RINA Consulting S.p.A. -* ***Claudio Ponzo,*** *Nissan Technical Centre Europe -* ***Prof. Marco E. Biancolini,*** *University of Rome "Tor Vergata"*

Structural Optimization: part 3

- Morphing is performed moving the external edge along x and y axes
- The body takes a C shape which increases stiffness

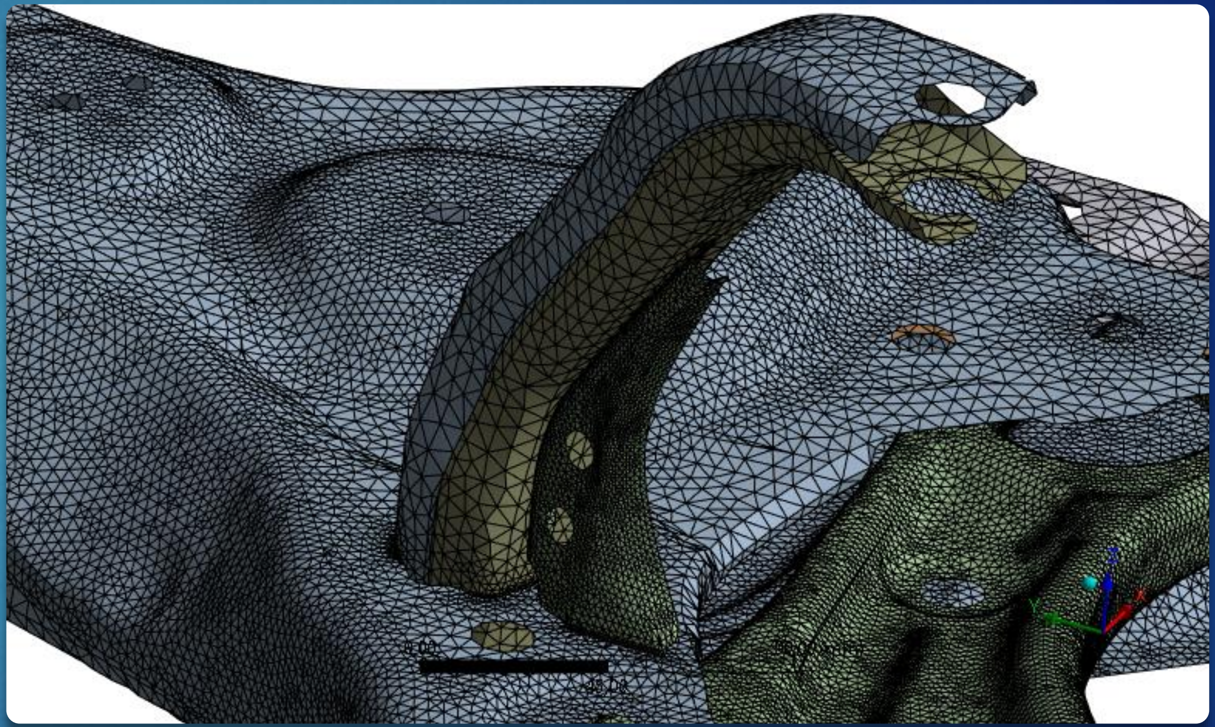

Structural Optimization: automation

- The previously shown modification are performed together in the final modified assembly, setting up automatic design exploration
- Central bush is replaced with a stiffer one: as the bush is a commercial part, a specific model was chosen, with no need for optimization.

	Name	Parameter type	Reference value	Constant	Resolution	Range		Range plot
1	Applied_Force_Y_Component	Optimization	-2755	☑	Continuous	-3030.5	-2479.5	
2	Midpoint__Delta_y	Optimization	20	☐	Discrete by value	0; 10; 20; 30		
3	Moving_Beads__Surface_Offset	Optimization	5	☐	Discrete by value	1; 2; 3; 4; 5		
4	Midpoint__Delta_x	Optimization	10	☐	Discrete by value	0; 10; 20; 30		
5	Applied_Force_X_Component	Optimization	0	☑	Continuous	-1	1	
6	MIDSURF_ASSEMBLY_PRL_Midsurface1_Thickness	Optimization	4	☐	Discrete by value	2; 2.5; 3; 3.5; 4		

Structural Optimization: automation

- The following parameters are set up in the automatic design exploration:
  - TV–Link reinforcement thickness
  - TV-Link beads surface offset
  - Q-Link edge midpoint delta X
  - Q-Link edge midpoint delta Y
- AMOP (Adaptive Metamodel of Optimal Prognosis) criterion is used

	Name	Parameter type	Reference value	Constant	Resolution	Range		Range plot
1	Applied_Force_Y_Component	Optimization	-2755	☑	Continuous	-3030.5	-2479.5	
2	Midpoint__Delta_y	Optimization	20	☐	Discrete by value	0; 10; 20; 30		
3	Moving_Beads__Surface_Offset	Optimization	5	☐	Discrete by value	1; 2; 3; 4; 5		
4	Midpoint__Delta_x	Optimization	10	☐	Discrete by value	0; 10; 20; 30		
5	Applied_Force_X_Component	Optimization	0	☑	Continuous	-1	1	
6	MIDSURF_ASSEMBLY_PRL_Midsurface1_Thickness	Optimization	4	☐	Discrete by value	2; 2.5; 3; 3.5; 4		

Optimization: final test

- The tests performed at different load conditions show a significant rise in stiffness measured on LVDT 2, while on LVDT 4 values there is a moderate increase and LVDT 7 values are almost unvaried
- This leads to put the lateral stiffness evaluated by LVDT4 as the parameter to maximize

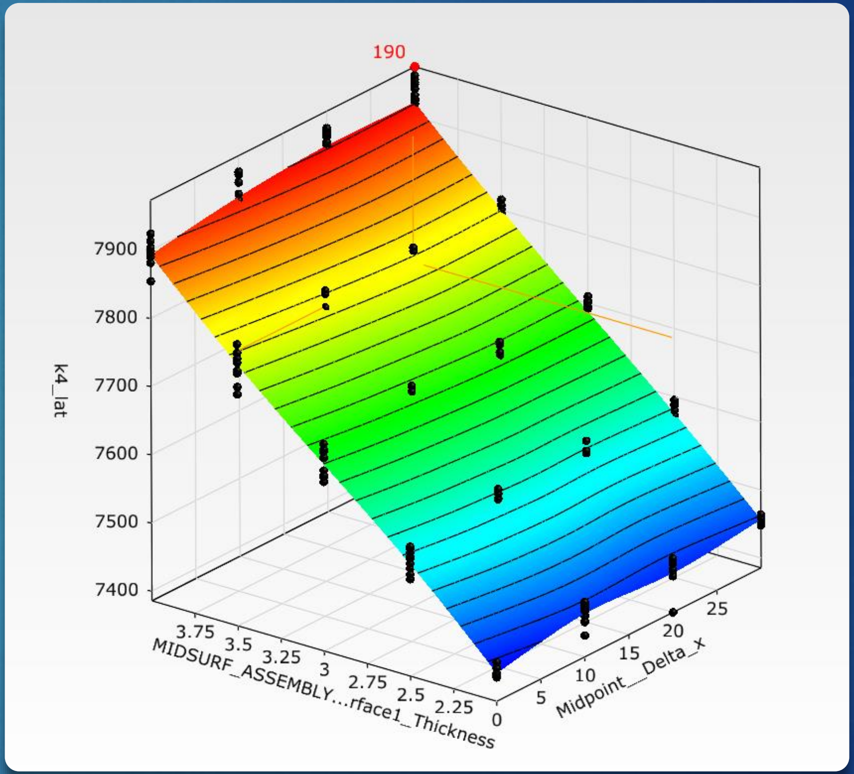

Optimization: final test

- The figures show the optimal point for k4 (stiffness measured by LVDT4) when a lateral load F = 2755 N is applied.
- Such a configuration shows good result also for k2 and k7

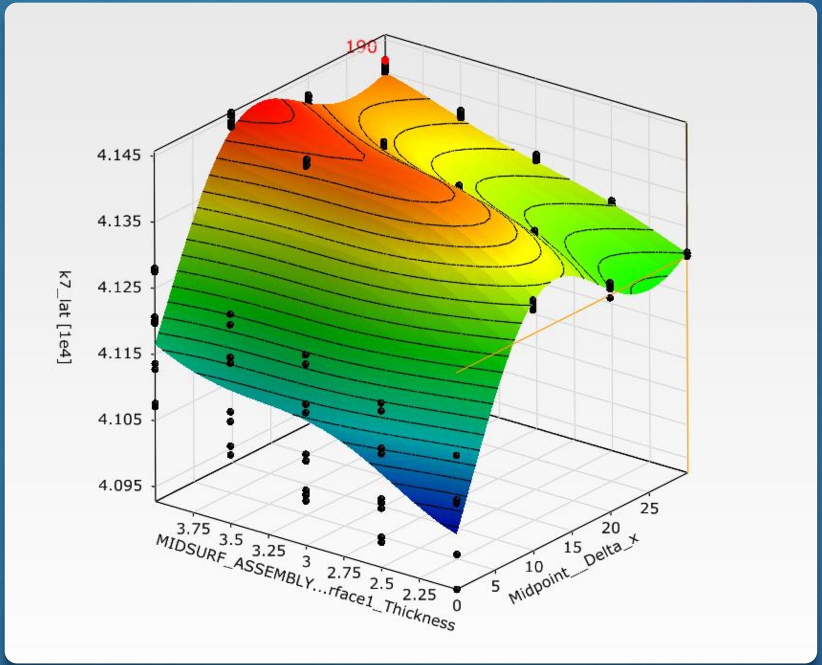

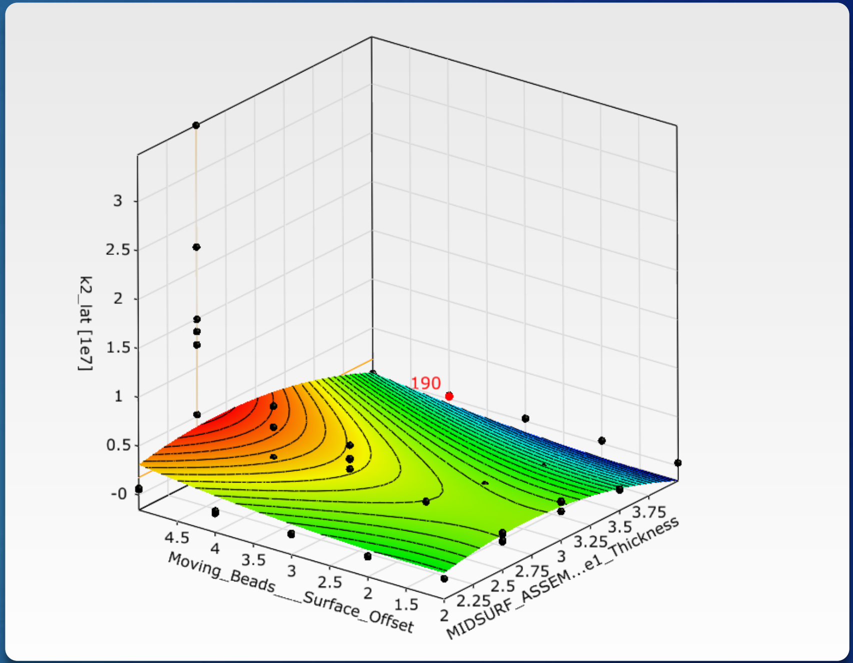

Optimization: final test

- A mean optimized condition was evaluated testing different geometry and load conditions.
- The final optimized geometry leads to the following values:
  - TV–Link reinforcement thickness: 4 mm
  - TV-Link beads surface offset: 4 mm
  - Q-Link edge midpoint delta X: 20 mm
  - Q-Link edge midpoint delta Y: 20 mm

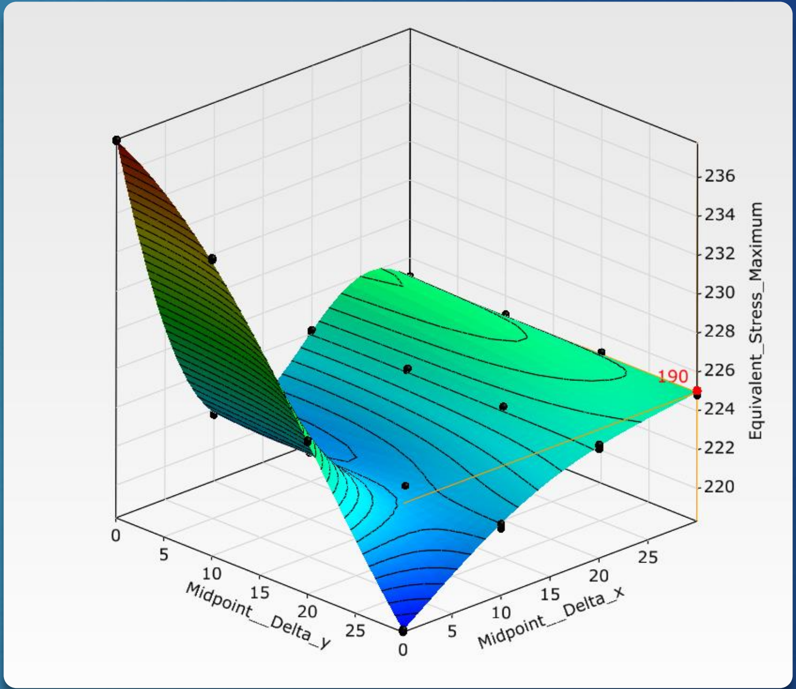

Optimization: final test

- The final optimized geometry leads to the following values:
  - TV–Link reinforcement thickness: 4 mm
  - TV-Link beads surface offset: 4 mm
  - Q-Link edge midpoint delta X: 20 mm
  - Q-Link edge midpoint delta Y: 20 mm
- Figure shows Equivalent Maximum Stress trend over the subframe surfaces

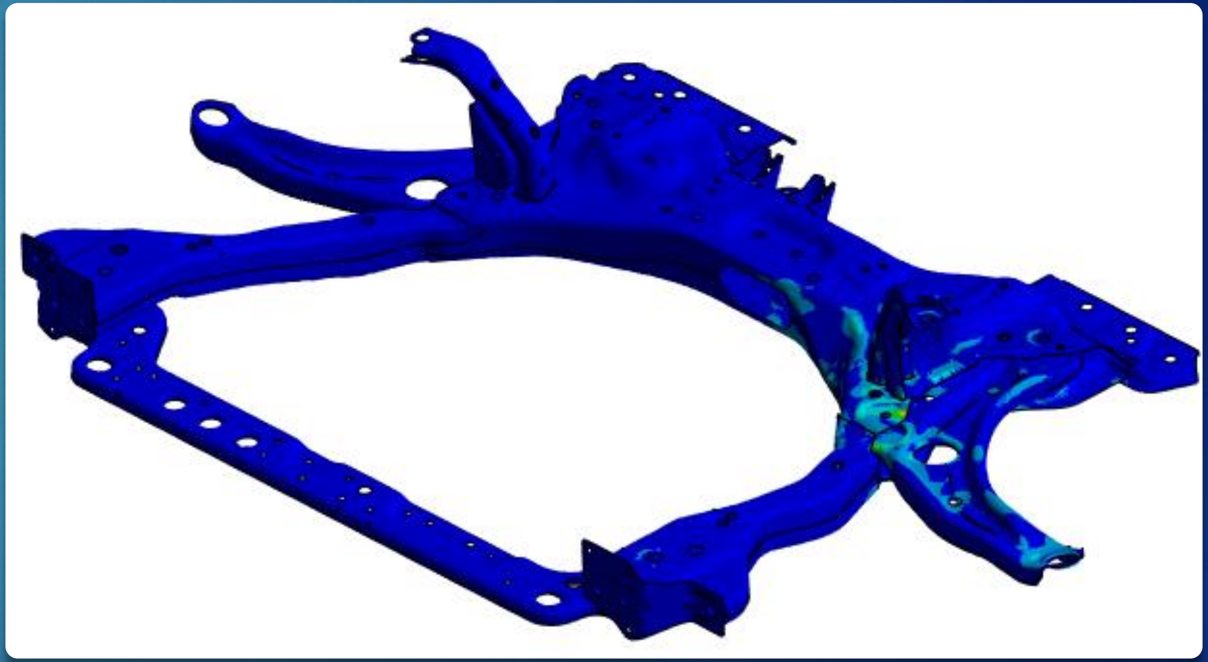

Optimization: final test

- The final optimized geometry leads to the following values:
  - TV–Link reinforcement thickness: 4 mm
  - TV-Link beads surface offset: 4 mm
  - Q-Link edge midpoint delta X: 20 mm
  - Q-Link edge midpoint delta Y: 20 mm
- Figure shows Total Deformation trend over the subframe surfaces

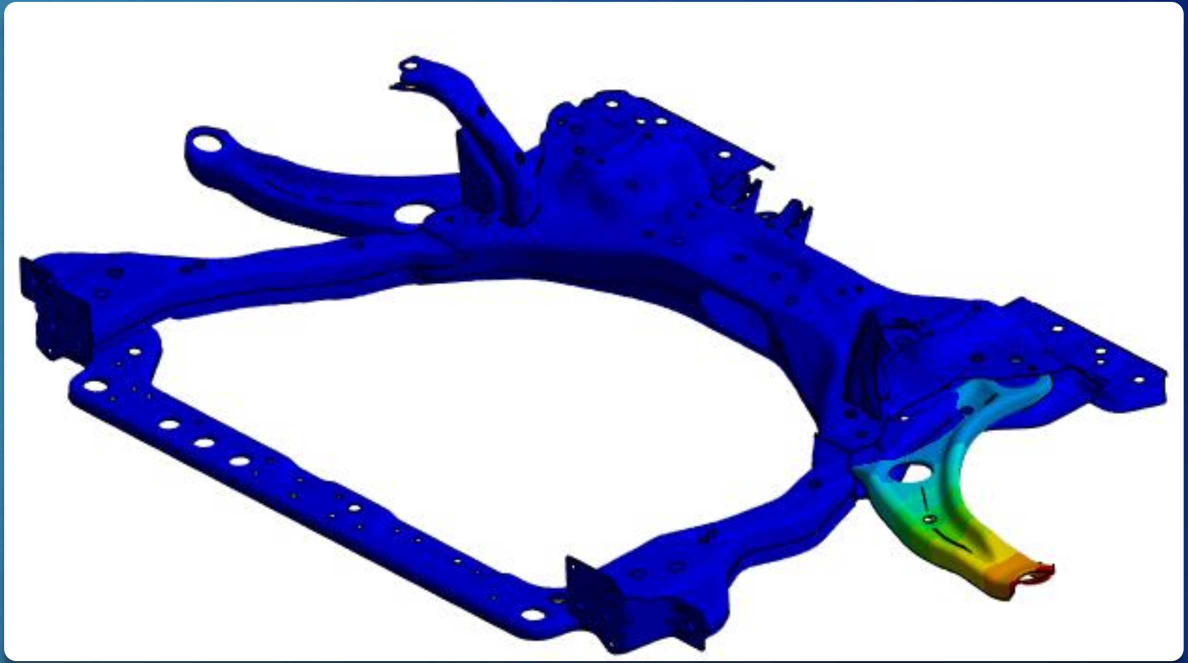

Results evaluation

- Lateral stiffness values are compared among competitor's car, Micra base and Micra optimized configuration
- Large increase in lateral stiffness is measured of the lower arm (LVDT 2)
- Lateral bushing stiffness is increased (LVDT 4), but not enough to reach competitor's value
- Front member (LVDT 7) lateral stiffness is almost unchanged

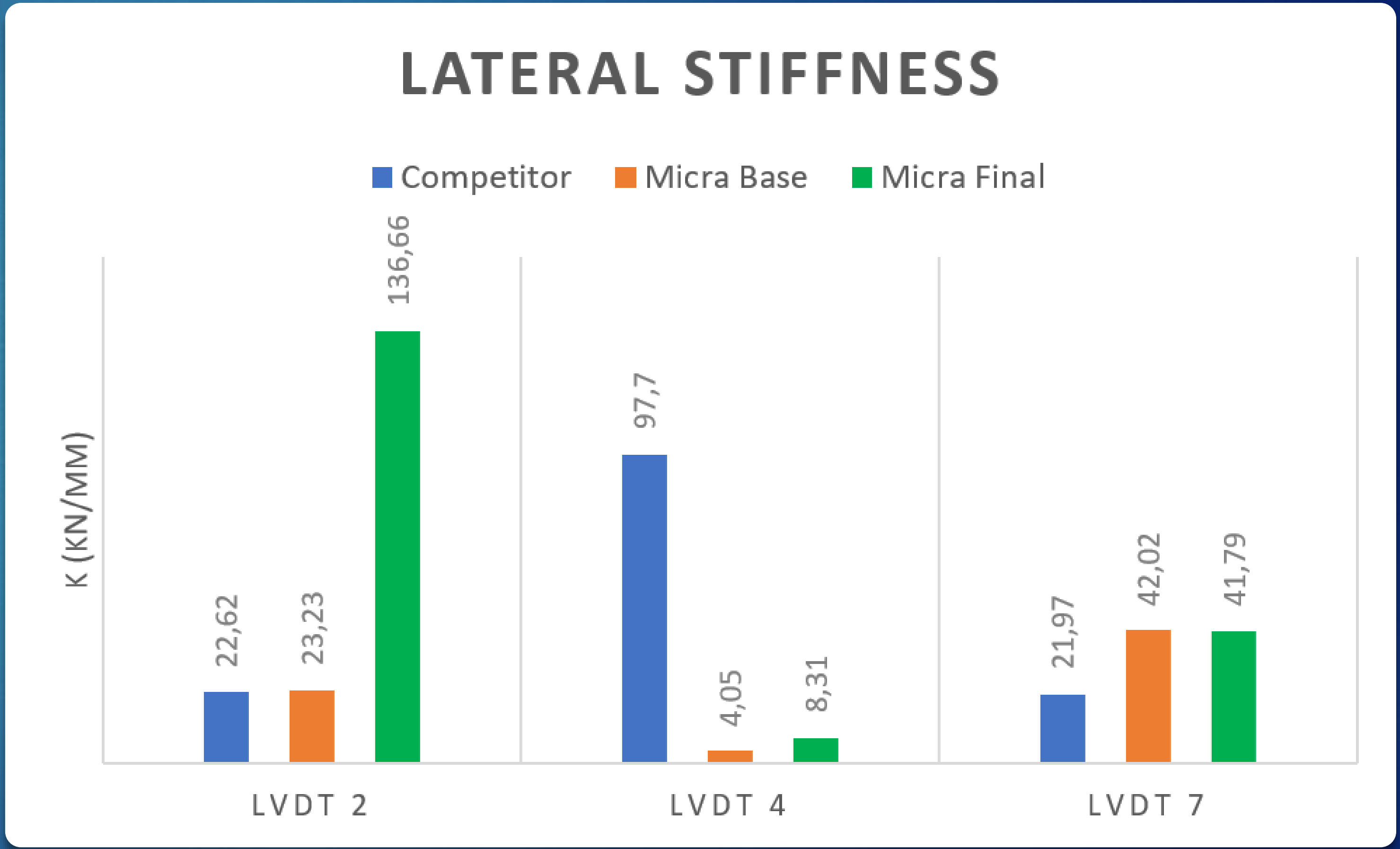

Results evaluation

- Similar behaviour in longitudinal load conditions compared to lateral load
- Lower arm becomes much stiffer, while longitudinal stiffness due to bushings doubles.
- Front member longitudinal stiffness also unchanged

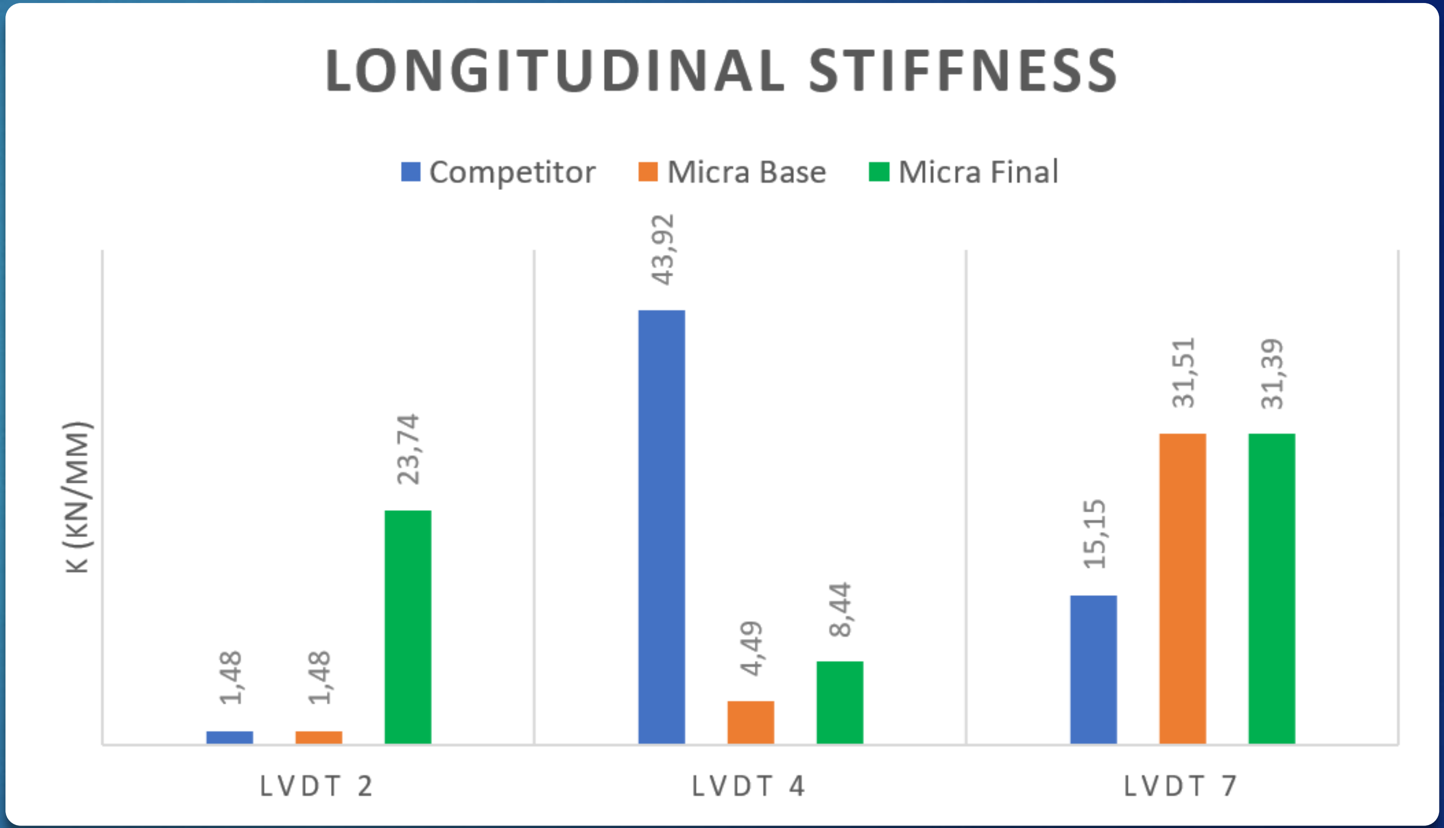

Conclusions

- A finite element analysis of a front subframe and connecting elements was performed
- Different optimization solutions were implemented to get a higher stiffness resulting in a final assembly with increased lateral stiffness
- Modifications carried to a small mass increase (0.5 kg) and a slight reduction in stress on lower arm

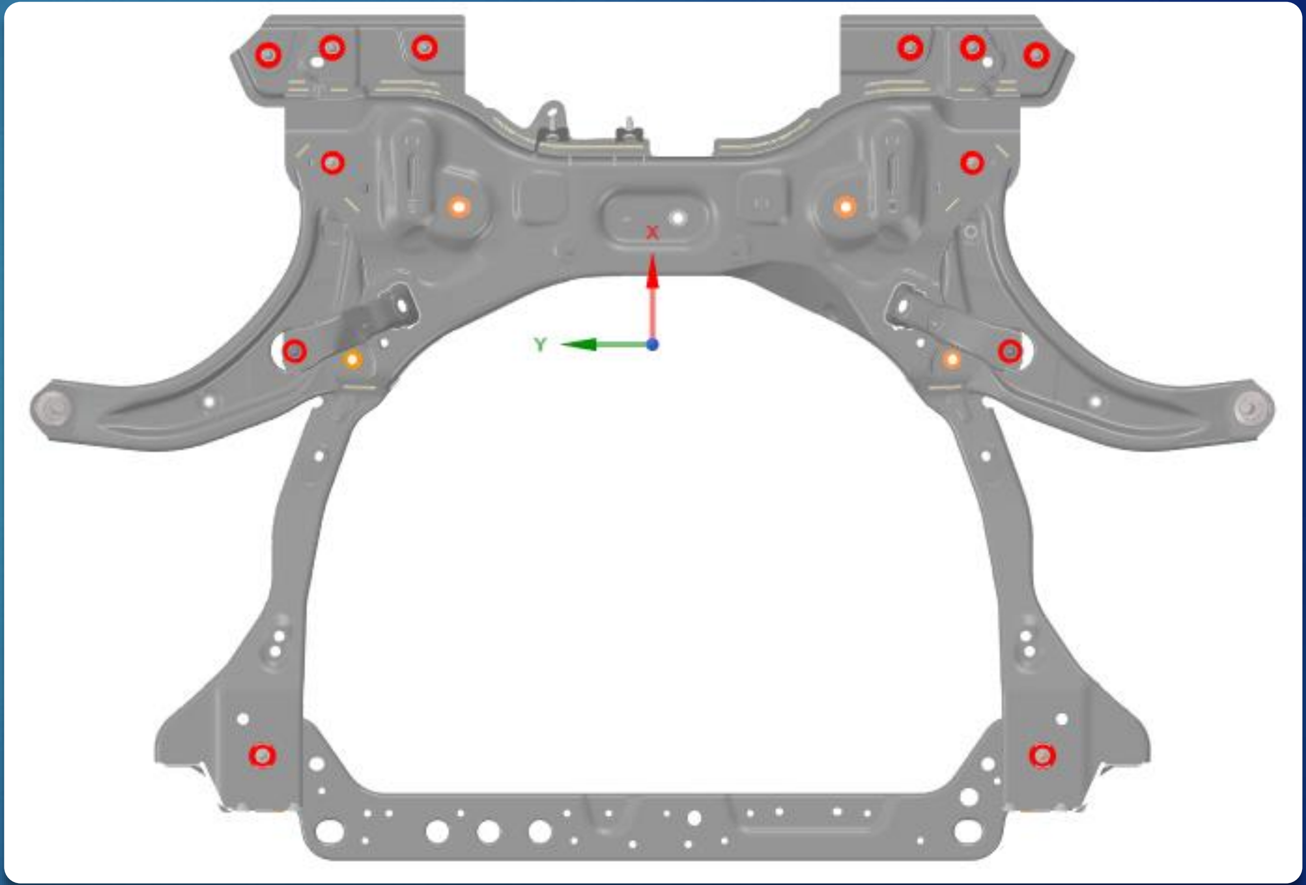

Emanuele Di Meo, *RINA Consulting S.p.A.* - ***Claudio Ponzo,*** *Nissan Technical Centre Europe* - ***Prof. Marco E. Biancolini,*** *University of Rome "Tor Vergata"*

Future Work

- Welds modeling, fatigue and vibrational analysis, to be implemented in structural optimization
- Technical and cost analysis of a change in material, for example using an aluminium subframe in place of a steel one, to get a remarkable mass reduction

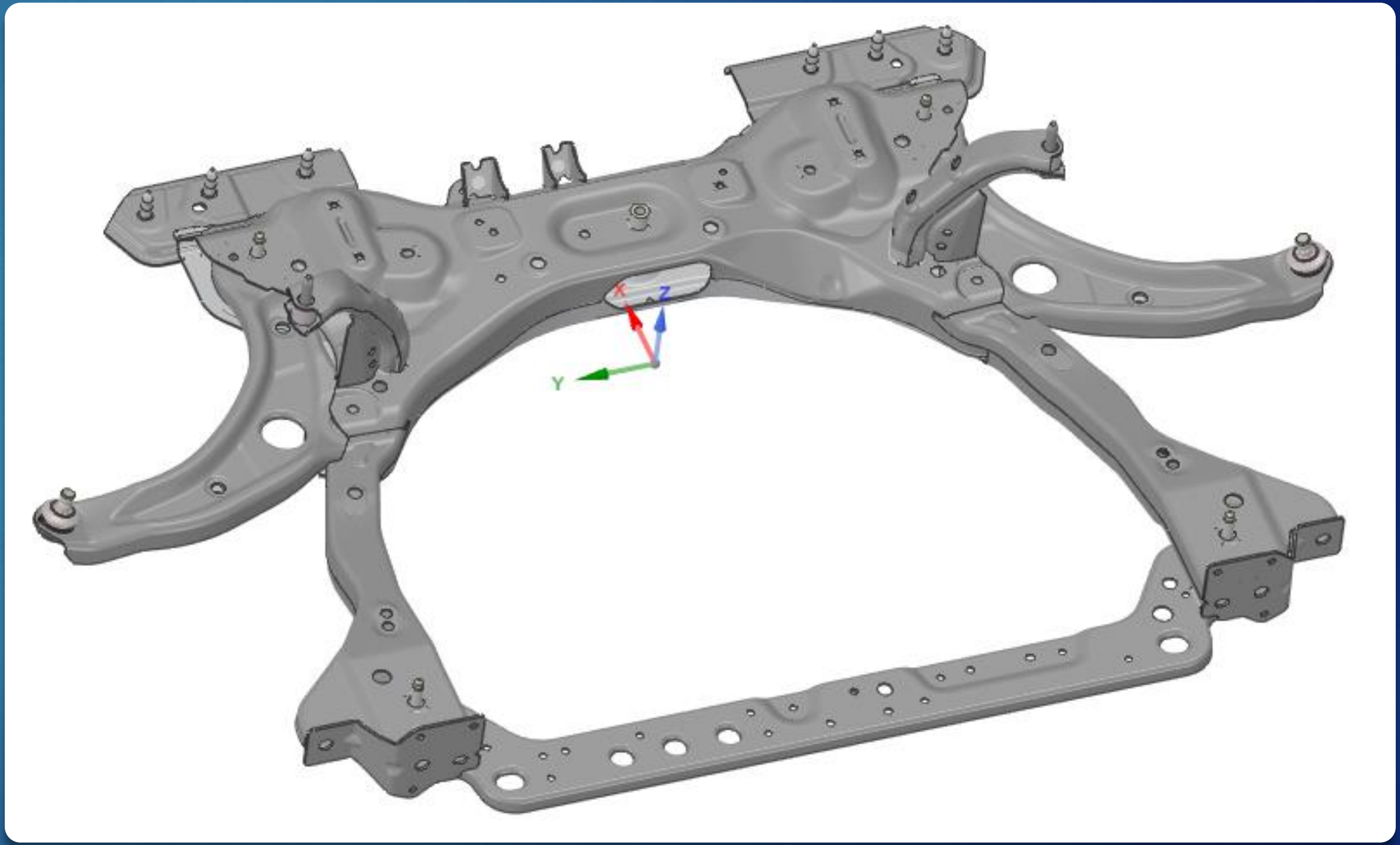

Maximilan Günther
Nissan e-DAMS
Rome e-Prix 2022
ABB FIA Formula E World Championship

Thank you for your attention

Emanuele Di Meo, *RINA Consulting S.p.A.*
Claudio Ponzo, *Nissan Technical Centre Europe*
Prof. Marco E. Biancolini, *University of Rome "Tor Vergata"*

38th International CAE Conference
November 16, 2022